JOURNAL OF GEOPHYSICAL RESEARCH, VOL. 96, NO. B9, PAGES 14,239–14,262, AUGUST 10, 1991

Paleomagnetism of the Moenkopi and Chinle Formations in Central New Mexico: Implications for the North American Apparent Polar Wander Path and Triassic Magnetostratigraphy

ROBERTO S. MOLINA-GARZA[1], JOHN W. GEISSMAN,[2] ROB VAN DER VOO,[1]
SPENCER G. LUCAS,[3] AND STEVE N. HAYDEN[2]

In central New Mexico, red sedimentary rocks unconformably overlying Permian carbonates of the San Andres Formation have been correlated with the Early-Middle Triassic Moenkopi and Late Triassic Chinle Formations of the Colorado Plateau. Paleomagnetic samples from Triassic sections exposed on basement cored uplifts along both the east and west side of the Rio Grande rift near Albuquerque yield, upon thermal and chemical demagnetization, well-defined, high unblocking temperature, dual-polarity magnetizations carried by hematite. The characteristic magnetization is interpreted as an early acquired chemical remanent magnetization based on a positive intraformational microconglomerate test and bedding-parallel magnetization polarity zonation. The Moenkopi and lowermost Chinle formations produced paleomagnetic poles respectively at 57.6°N-100.3°E (N=36 sites, K=74.1, A_{95}=2.8°) and 60.8°N-88.9°E (N=17 sites, K=130.3, A_{95}=3.1°). These data plus previously published and additional results from the underlying Permian strata suggest that portions of central New Mexico have experienced a small clockwise rotation (i.e., less than 10°) similar to that of the Colorado Plateau with respect to the North American craton. The paleomagnetic directions of the Chinle Formation and related strata in eastern New Mexico document about 12° (great circle distance) of rapid apparent polar wander during mid-Carnian to late Norian times along a track which contains other cratonic poles of similar age. We present a preliminary magnetic polarity time scale for the Triassic that incorporates the present New Mexico data and previously published data, mostly form continental red bed sequences. This magnetic polarity scale provides a basic framework which can be tested with future data from Triassic sections where additional biostratigraphic control exists.

INTRODUCTION

The Triassic continental red bed sequences of the western and southwestern United States have been the subject of considerable paleomagnetic research for over three decades [*Runcorn*, 1956; *Helsley*, 1969; *Helsley and Steiner*, 1974; *Baag and Helsley*, 1974; *Van der Voo and Grubbs*, 1977; *Elston and Purucker*, 1979; *Purucker et al.*, 1980; *Walker et al.*, 1981; *Larson and Walker*, 1982; *Herrero-Bervera and Helsley*, 1983; *Shive et al.*, 1984; *Bazard and Butler*, 1989]. These studies have led to a well-determined Triassic segment of the North American apparent polar wander path (APWP) [*Gordon et al.*, 1984]. Nonetheless, recently published Middle-Late Triassic paleopoles from New England [*Fang and Van der Voo*, 1988] and Nova Scotia [*Symons et al.*, 1989] are located at lower latitudes, away from the generally accepted APWP segment as determined mostly from localities in southwest North America. Likewise, paleomagnetic poles from the early Mesozoic rift basins in the northeastern United States (e.g., the Newark Supergroup) are consistently located to the east of poles obtained from units in southwest North America thought to be of the same age (Chinle Formation and related strata).

Discrepancies among paleopole determinations can be explained in several ways. They may be due to errors derived from incomplete removal of secondary magnetizations, partially incorrect stratigraphic correlations (particularly in continental red beds which often lack adequate biostratigraphic control), undetected rotations or structural complexity (leading to errors in determining the paleomeridian or the paleo-horizontal), or long term deviations of the geomagnetic field from a geocentric axisymmetric dipole. Finally, a more irregular distribution of paleopoles may, in fact, represent a truly more complex APWP than previously assumed.

Progress was made in recent years when previously proposed models involving a Mesozoic to early Tertiary clockwise rotation of the Colorado Plateau were evaluated [*Steiner*, 1986; *Bryan and Gordon*, 1986]. These studies have shown that paleomagnetic poles derived from the Colorado Plateau require a small (e.g., 5°-11°) correction before they can be compared with poles from the stable craton. This correction affects the location of the paleopole mostly in longitude; thus, latitudinal differences still remain unexplained.

Aspects regarding the nature, time of remanence acquisition, and fidelity of the magnetic record in red beds have been strongly debated by authors with quite contrary views. In particular, studies of the Triassic Moenkopi Formation by *Walker et al.* [1981] have shown that a significant fraction of the iron oxides in red beds are unequivocally of diagenetic origin. This, and other petrographic, rock magnetic and paleomagnetic observations led *Larson et al.* [1982] to propose a model for long-term-acquisition of chemical remanent magnetizations (CRM) in red beds. Consequently, paleomagnetic results derived from red beds may be considered less reliable in the sense that they may not record the direction and polarity of the field at the specific time of deposition. Thus, *Larson et al.* [1982] argued that red beds can record a resultant of directions

[1]Department of Geological Sciences, University of Michigan, Ann Arbor.
[2]Department of Geology, University of New Mexico, Albuquerque.
[3]New Mexico Museum of Natural History, Albuquerque.

Paper number 91JB00644.
0148-0227/91/91JB-00644$05.00

and polarities acquired over a period spanning several million years. In contrast, studies by *Elston and Purucker* [1979], also of the Moenkopi Formation, provide evidence for a detrital remanent magnetization (DRM) or, at worst, an early acquisition of a CRM. These conclusions are supported by a bedding inclination error anomaly in foreset-bottomset layers and other observations (positive intra-formation conglomerate test, soft-sediment-deformation fold test, and layer-parallel magnetic polarity zones). The two groups of workers, however, have failed to provide a complete characterization of the remanent magnetization of the unit studied by disregarding the nature and stability of secondary remagnetizations.

A provisional Early to Middle Triassic magnetic polarity sequence has also been compiled and correlated with relative success across the western United States [*Lienert and Helsley*, 1980; *Shive et al.* 1984]. While the use of red beds in magnetostratigraphic problems is still debated, recently published results from Early Triassic carbonate sequences from southern China [*Steiner et al.*, 1989] and red beds from central Spain [*Turner et al.*, 1989] provide independent magnetic polarity sequences with which the North American data can be compared.

Here, we present paleomagnetic data for continental red beds assigned to the Moenkopi and Chinle formations, exposed off and along the eastern margin of the Colorado Plateau in the Rio Grande rift area in central New Mexico.

GEOLOGY AND SAMPLING

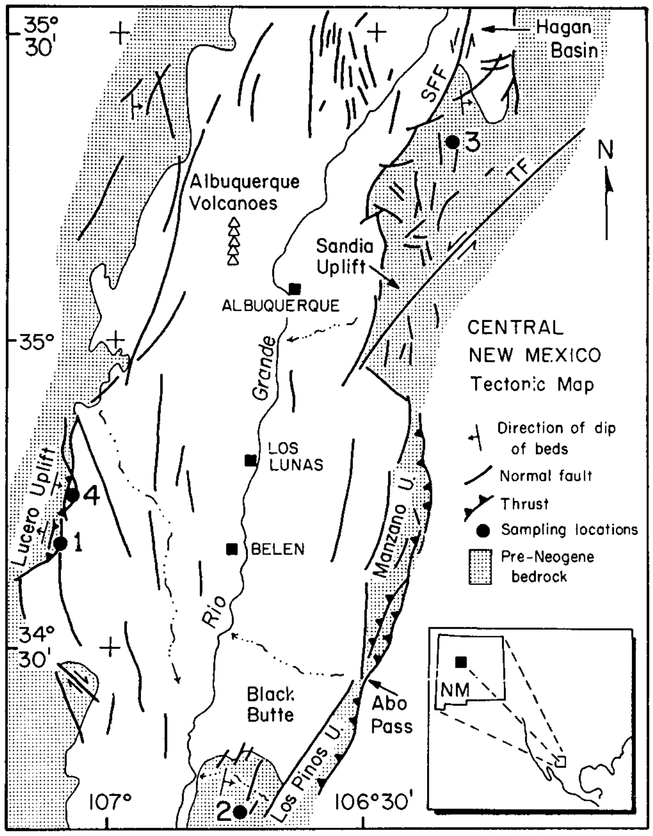

Fig. 1. Simplified tectonic map of central New Mexico [after *Kelley*, 1979] showing sampling locations: (1) Mesa Gallina, (2) Sevilleta Grant, (3) Tejon, (4) Carizo Arroyo. SFF, San Francisco Fault; TF, Tijeras Fault.

A relatively well exposed section of continental red beds in the Rio Grande rift area, in central New Mexico (Figure 1), has been correlated with and assigned to the Lower-Middle Triassic Moenkopi and Upper Triassic Chinle Formations as defined on the Colorado Plateau [*Stewart et al.*, 1972a, b; *Lucas and Hayden*, 1989]. Correlation is based on the stratigraphic position of the sequence, paleontological data, and lithostratigraphic correlations. The Triassic sequence disconformably overlies Permian carbonate and clastic strata and is in turn covered by Middle-Upper Jurassic or younger rocks (Figure 2). The Moenkopi Formation in central New Mexico is relatively thin (maximum thickness 70m). It consists of alternating and interfingering layers of immature sandstone (litharenites and lithic wackes), siltstone, and mudstone, ranging in color from purple to grayish-red and reddish-brown; small-scale trough cross beds and laminar bedding are common. The age of the Moenkopi Formation in central New Mexico is latest Early (?) to Middle Triassic on the basis of vertebrate fossils and microfossils [*Lucas and Hayden*, 1989; *Kietzke*, 1989]. The vertebrate fossils include three partial vertebrae and most of the scapula of a non-parasuchian thecodont reptile, and one partial interclavical armor plate from a capitosauroid amphibian. Microfossils (ostracodes and charophytes) also indicate an Early to Middle Triassic age, suggesting correlation of these strata with the Holbrook Member of the Moenkopi Formation of northeastern Arizona and the Moody Canyon Member of southeastern Utah [*Lucas and Hayden*, 1989]. The Holbrook Member has produced a Middle Triassic vertebrate fauna [*Morales*, 1987]. The Moenkopi Formation in central New Mexico has also been correlated with the Anton Chico Member of the Moenkopi Formation of the Tucumcari basin of east-central New Mexico [*Lucas and Hunt*, 1987, 1989b]. *Lucas and Hunt* [1987] have argued a Mid-Triassic age for the Anton Chico based on the presence of capitosauroid amphibians. This further supports a Middle Triassic age (241-235 Ma) for the Moenkopi Formation in central New Mexico.

Rocks assigned to the Chinle Formation in central New Mexico locally exceed several hundred meters in thickness. The contact between the Moenkopi and Chinle formations is a disconformity marked either by "mottled strata" or by a quartz-pebble conglomerate and quartzose sandstones that are correlative with the Shinarump Member of the Chinle Formation on the Colorado Plateau [*Lucas and Hayden*, 1989; *Lucas et al.*, 1988; *Hunt and Lucas*, 1988b]. The Chinle Formation consists of mostly light brown, pale reddish-brown, and grayish-red claystone, grading to siltstone, sandstone (locally conglomeratic) and greenish gray lacustrine limestone (the informal Ojo Huelos limestone bed) [*Lucas et al.*, 1988; *Lucas and Hayden*, 1988, 1989]. A zone of "mottled-strata", generally no more than a few meters thick, occurs in the upper beds of the Moenkopi and the basal strata of the Chinle formation. The "mottled-strata" (a pedogenic horizon [*Stewart et al.*, 1972a]) consist of peculiar reddish purple siltstone layers mottled by greenish gray light patches. In west-central New Mexico the Chinle Formation is represented by the Shinarump Member, the Bluewater Creek Member (formerly Monitor Butte Member), and the Petrified Forest Member. The units of the Chinle Formation sampled in the present study belong to the Shinarump-Agua Zarca Members and an overlying (locally) unnamed member which we will call Bluewater Creek Member because they are correlative. The Ojo Huelos limestone bed [Lucas et al., 1988] is a pisolitic and fenestrate,ostracodal limestone and yellowish-gray sandy mudstone unit within this

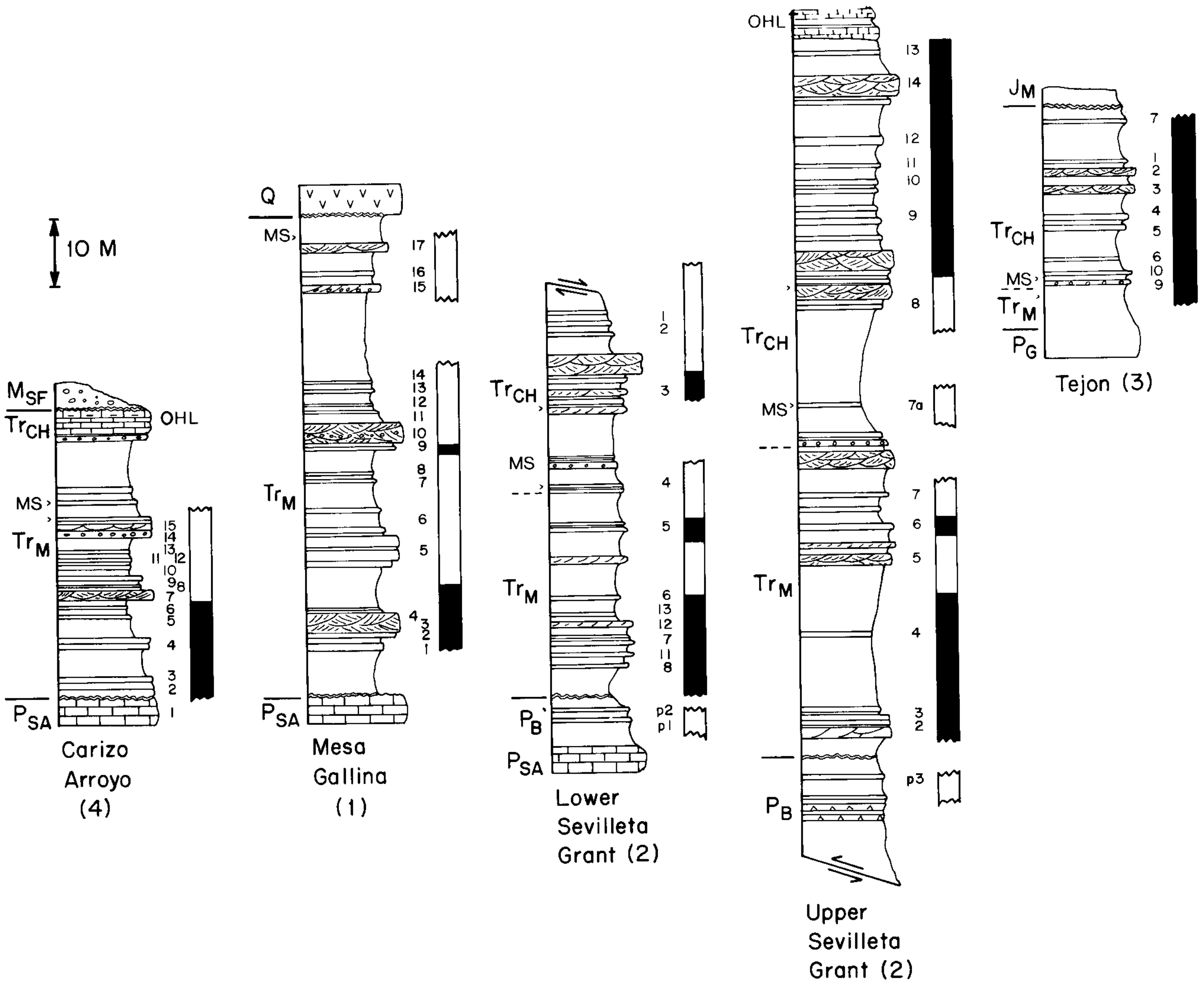

Fig. 2. Schematic stratigraphic sections for the Triassic sequence in central New Mexico. Paleomagnetic sites and magnetic polarity sequences are shown to the right of each column. Two columns are shown for Sevilleta Grant, corresponding to blocks separated by a north-south trending normal fault. P_{SA}, Permian San Andres; P_B, Late Permian Bernal; P_G, Permian Glorieta; Tr_M, Triassic Moenkopi; Tr_{CH}, Triassic Chinle; J_M, Middle Jurassic; M_{SF}, Miocene Santa Fe; Q, Quaternary Basalt; MS>, Mottled strata; OHL, Ojo Huelos Limestone.

unnamed member. It contains Late Triassic fossils that include the skull of a large metoposaurid labyrinthodont, phytosaur teeth, a microfauna of fish teeth (including the freshwater Late Triassic shark *Lissodus*), and the darwinulid ostracodes *Darwinula* sp. and *Gerdalia* cf. *G. Triassica*. Rocks assigned to the Bluewater Creek (unnamed) member of the Chinle Formation in central Mew Mexico correlate in part with the Monitor Butte Member in southern Utah, the Santa Rosa Formation in eastern New Mexico and the Popo Agie Formation in Wyoming [*Lucas and Hunt*, 1989a; A.P. Hunt and S.G. Lucas, The *Paleorhinus* bichron and the correlation of the nonmarine Upper Triassic of Pangea, submitted to *Paleontology*, 1990]. Stratigraphic correlations of Late Triassic strata in east and central New Mexico and the Colorado Plateau are shown in Figure 3.

Based on a correlation of the plant megafossil zonation of North American rocks with the Triassic stages in Germany (using associated pollen and spores) the Shinarump and Monitor Butte (now called Bluewater Creek) members of the Chinle Formation in Utah, Arizona, and western New Mexico have been assigned a middle Carnian age [*Ash*, 1980]. This correlation, however, has been disputed by *Lupe and Silberling* [1985] who have correlated depositional cyclicity of the Chinle Formation in Utah, with major terrigenous clastic influx events into the basin of deposition of the Auld Lang Syne Group in northwest Nevada. Marine carbonates from the Auld Lang Syne Group have a relatively well established Norian age. These authors then favor a Norian age for deposition of the Chinle Formation in Utah. In New Mexico, the late Carnian age of the base of the Chinle is supported by the occurrence of the phytosaur *Paleorhinus* which is also known from well-established late Carnian (Tuvalian) marine strata in Austria (A.P. Hunt and S.G. Lucas, submitted manuscript, 1990). Moreover, *Hunt and Lucas* [1988a] have described a vertebrate fauna of late Carnian age from the Los Esteros Member of the Santa Rosa Formation of the Tucumcari basin of East-central New Mexico. Correlation of the Santa Rosa and Shinarump strata (Figure 3) indicates a late Carnian age for the latter. A

	Tucumcari Basin	Central New Mexico	Colorado Plateau
			Rock Pt. Member
Norian	Redonda Formation	Redonda Member	
			Owl Rock Member
	Bull Canyon Formation	Upper Petrified Forest	
———	Trujillo Formation	Sonsela	
		Lower Petrified Forest	
Carnian	Garita Greek Formation	Unnamed Bluewater Creek	Monitor Butte
	Santa Rosa Formation	Agua Zarca Shinarump	Mottled Strata

Fig. 3. Stratigraphic correlation of the Chinle Formation and related strata in southwestern United States.

late Carnian fauna has also been recovered from the Garita Creek Formation which overlies the Santa Rosa Formation and has been correlated with the lower Petrified Forest Member of the Chinle Formation [*Hunt et al.*, 1989]. Thus, rocks assigned to, or correlated with, the Chinle Formation in New Mexico sampled in the present study are entirely restricted to the Carnian.

We sampled four stratigraphic sections near Albuquerque, which are part of Cenozoic-age basement-cored uplifts that expose late Paleozoic and Mesozoic strata on both the east and west side of the Rio Grande rift. Sampling localities are shown in Figure 1 and stratigraphic columns, including paleomagnetic sampling levels, in Figure 2. At Mesa Gallina, a relatively intact, gently west dipping Triassic section disconformably overlies the Late Permian San Andres Limestone of the Artesia Group and is situated west of a series of late Cenozoic, rift-related, faults which define the Lucero Uplift. At Carizo Arroyo, north of the Mesa Gallina locality, the Triassic section sampled also disconformably overlies the San Andres Limestone, but here it lies in the hanging-wall of a series of late Cenozoic normal faults and dips moderately eastward. At Sevilleta Grant, in the Joyita Hills, the section is repeated as a result of motion along a north-south trending normal fault of Cenozoic age. The base of the section, where the Moenkopi Formation disconformably overlies the Permian "Bernal Formation" (Artesia Group), is thus exposed twice. Along the southwest margin of the Hagan basin near the ghost town of Tejon, "mottled strata" and the Agua Zarca Member of the Chinle Formation rest disconformably on a thin section of Moenkopi which overlies the Late Permian Glorieta Sandstone of the Artesia Group.

A total of 75 paleomagnetic sites were sampled in the field, each from a single stratigraphic horizon, preferentially of fine-grained sandstone and siltstone. Samples were obtained with a portable drill and oriented with both magnetic and sun compasses. In the laboratory, 2.1 cm long specimens were prepared from each sample.

PALEOMAGNETIC DEMAGNETIZATION ANALYSIS

Natural remanent magnetization (NRM) measurements were made with a ScT cryogenic magnetometer in a magnetically shielded room at the paleomagnetic laboratory of the University of Michigan. NRM intensities are moderately high. Eighty-five percent of the samples have intensities between 1 and 10 mA/m; the full range of variation is between 0.2 and 475 mA/m. The bulk of the NRM directions form two nearly antipodal groups of directions with northerly and southerly declinations and shallow inclinations; other directions plot in the lower hemisphere along a streak roughly parallel to the north-south meridian. NRM directions from the Tejon section are well clustered east of north at shallow inclinations.

A relatively small and randomly distributed magnetization component, possibly acquired during sampling and handling, was removed by washing the samples in diluted HCl for a few seconds before further treatment. The NRM was studied by conventional stepwise alternating field (AF), thermal, and chemical demagnetization techniques. AF and thermal demagnetization were performed in 10 to 20 incremental steps up to a maximum induction field of 100 mT and temperature of 690°C, using Schonstedt instrumentation. Chemical demagnetization was carried out in ambient field using concentrated HCl at 60°C; samples were then rinsed and dried in a reduced induction space (less than 10 nT) before measurement.

Figure 4 shows typical orthogonal demagnetization diagrams [*Zijderveld*, 1967]. The majority of the specimens are characterized by relatively simple behavior upon demagnetization. Thermal demagnetization diagrams generally reveal nearly univectorial decay of the magnetization (Figures 4a and 4b) or two magnetization components with only partially overlapping unblocking temperature spectra. The magnetic vector removed first has northerly to easterly declinations and steep downward inclinations (Figures 4c and 4d). Generally, this component has relatively high laboratory unblocking temperatures (between 25°C and 620°C). However, thermal demagnetization at low temperatures (i.e., 50°, 70°, 100°, and 150°C steps) suggests that a significant portion of the northerly component is carried by goethite. The low temperature component forms well-defined linear segments in demagnetization diagrams (Figures 4*c* and 4*d*), suggesting isolation of a single magnetization. At some sites only northerly or easterly steep to moderate positive (or both) directions were observed. Neither chemical, thermal nor AF demagnetization allowed isolation of the characteristic magnetization in those sites.

The second component removed has shallow up (or downwards) inclination, and south-southeasterly (or north-northwesterly) declinations, except at Tejon where the declinations are directed to the north-northeast. Typically this magnetization unblocks at temperatures between 580°C and 690°C (Figure 4). This component is considered the formation characteristic magnetization. Thermal and chemical demagnetization are usually effective in isolating the characteristic (shallow) magnetization and removing the secondary (steep) overprints (Figures 4*a*, - *c*). However, some samples showed either slightly erratic behavior above 630°C or rather rapid decay of the magnetization above this temperature (Figure 4d, sample c52-1). This is possibly due to thermal instability of the magnetization carriers and/or formation of secondary magnetic phases from silicate minerals or preexisting oxide minerals. The characteristic direction of these samples was estimated using great circle trajectories. In those samples, chemical demagnetization alone produces curved demagnetization diagrams (indicating simultaneous removal of two components; see Figure 4*d*, sample c51). An alternative method involved treating unstable samples thermally up to 600-640°C, when secondary components were completely removed, and perform chemical demagnetization from there onwards. This method yields excellent results (Figure 4*d*, sample c52), producing well-defined linear decay of the

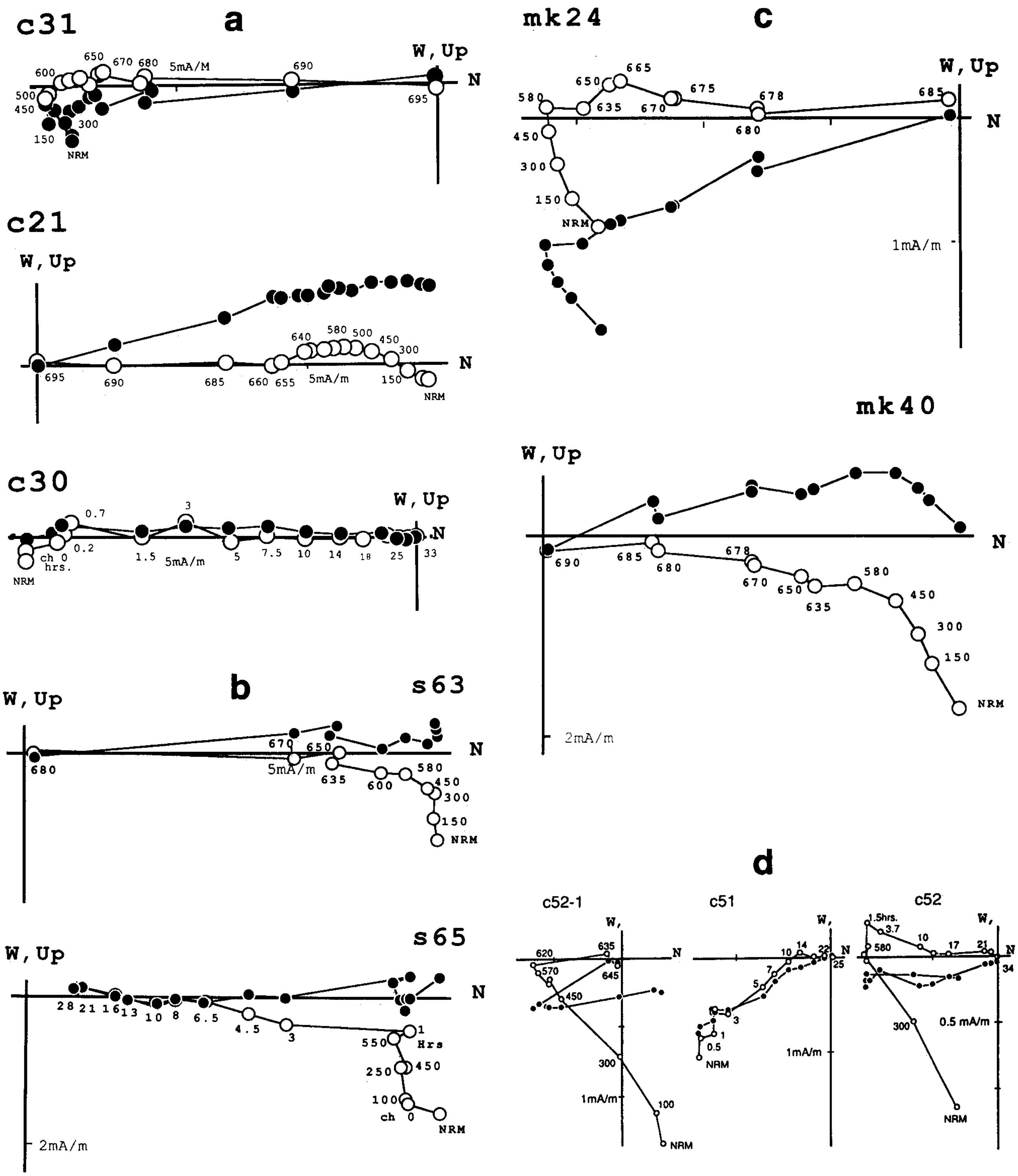

Fig. 4. Representative orthogonal demagnetization diagrams [*Zijderveld*, 1967]. The horizontal (vertical) projection is shown as solid (open) symbols. Temperatures are in degrees Celsius; for chemical demagnetization the time is given in hours. (*a*) Chemical and thermal demagnetizations in the Moenkopi Formation. (*b*) Chemical and thermal demagnetizations in the Chinle Formation. (*c*) Two-component magnetizations in the Moenkopi Formation separated by thermal demagnetization. (*d*) Two-component magnetizations in the Moenkopi Formation separated by thermal and chemical demagnetization combined.

characteristic magnetization (in contrast to chemical or thermal demagnetization alone).

AF demagnetization results in only a small decrease in intensity. It removes a generally northerly, but sometimes easterly, downward magnetization component. A few samples from site t8 are exceptional in the sense that intensities are as high as 400 mA/m. A peak induction of 10 mT during AF demagnetization reduces this strong NRM to less than 5% of its initial value. In thermal demagnetization of these samples, large intensity reductions are observed at about 580°C, and the

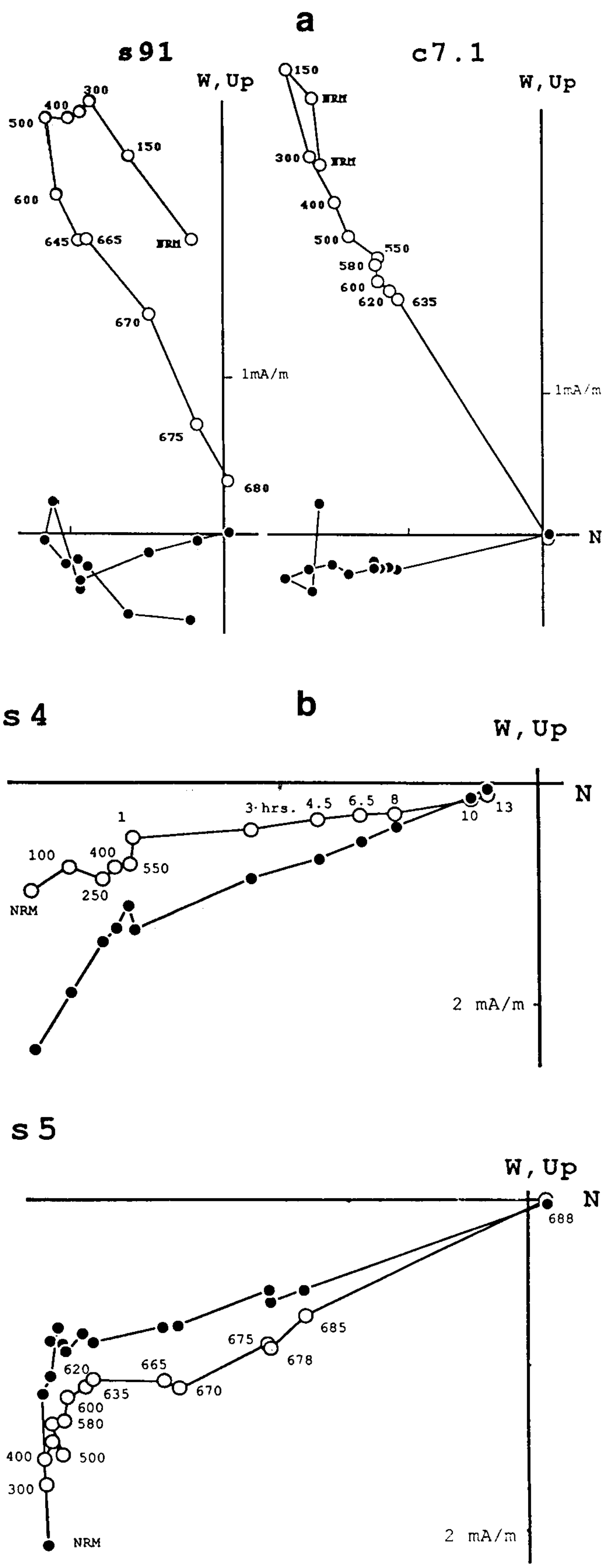

Fig. 5. (*a*) Examples of samples characterized by a southerly and relatively steep negative component of magnetization. (*b*) Univectorial decay of the remanence (above 600°C) of samples from the Permian red beds at Sevilleta Grant. Symbols as in Figure 4.

magnetization removed is nearly parallel, although slightly more northerly, to the still higher unblocking temperature characteristic magnetization. Samples from this site are also characterized by heavy mineral laminations. Ocasionally, AF demagnetization removes the characteristic magnetization in non red, presumably bleached, zones within the mottled strata.

Sites t9, s13-15, c2, and some samples from other sites, are characterized by a well-defined southeasterly and relatively steep upwards direction (Figure 5*a*). Unblocking temperatures for this component range between 300° and 680°C. Attempts to isolate the characteristic north-south shallow magnetization in those sites were not successful.

Three sites from the Late Permian "Bernal Formation" red beds underlying the Triassic section at Sevilleta Grant yield stable nearly univectorial magnetizations with laboratory unblocking temperatures above 600°C, with (tilt corrected) southeasterly shallow-upward directions (Figure 5b).

ROCK MAGNETISM AND ORE MICROSCOPY

Acquisition experiments of isothermal remanent magnetization (IRM) are presented in Figure 6. Normalized IRM acquisition curves are shown for three pairs of thermally demagnetized and HCl leached specimens, either from the same site or the same sample. None of the curves show saturation at 1.5 T indicating that the magnetic mineralogy is dominated by a high coercivity phase. IRM acquisition curves of leached samples show a progression towards a behavior similar to that of a non-red specimen from the mottled strata that responded well to AF treatment (s31). It is therefore very likely that a lower coercivity phase is also present, in small quantity. Only in a few sites does it carry a significant fraction of the remanence. At least one (unleached) sample shows a concave-up IRM curve, perhaps indicating the presence of goethite. High unblocking temperatures and coercivities suggest that hematite is the principal magnetic carrier of the well-defined magnetizations observed, except for the fraction removed at about 130°C (which is likely to be carried by goethite) and the low coercivity component observed in site t8.

Observations of polished samples under the reflected light microscope and scanning electron microscope indicate that

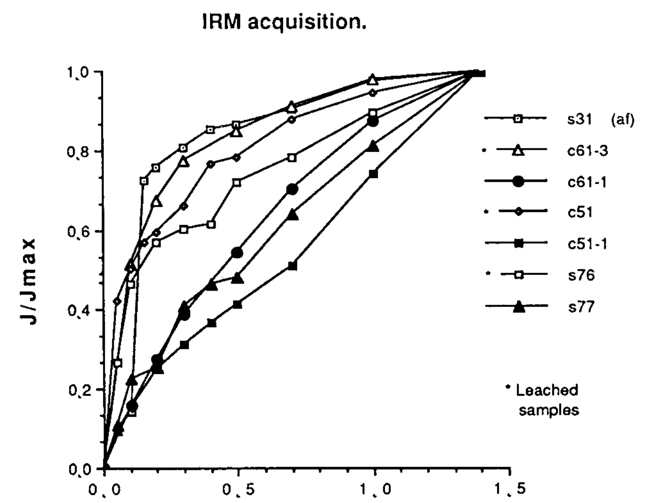

Fig. 6. Isothermal remanent magnetization acquisition diagrams of selected samples. Sample s31 is a nonred sample within the mottled strata which responded well to AF demagnetization.

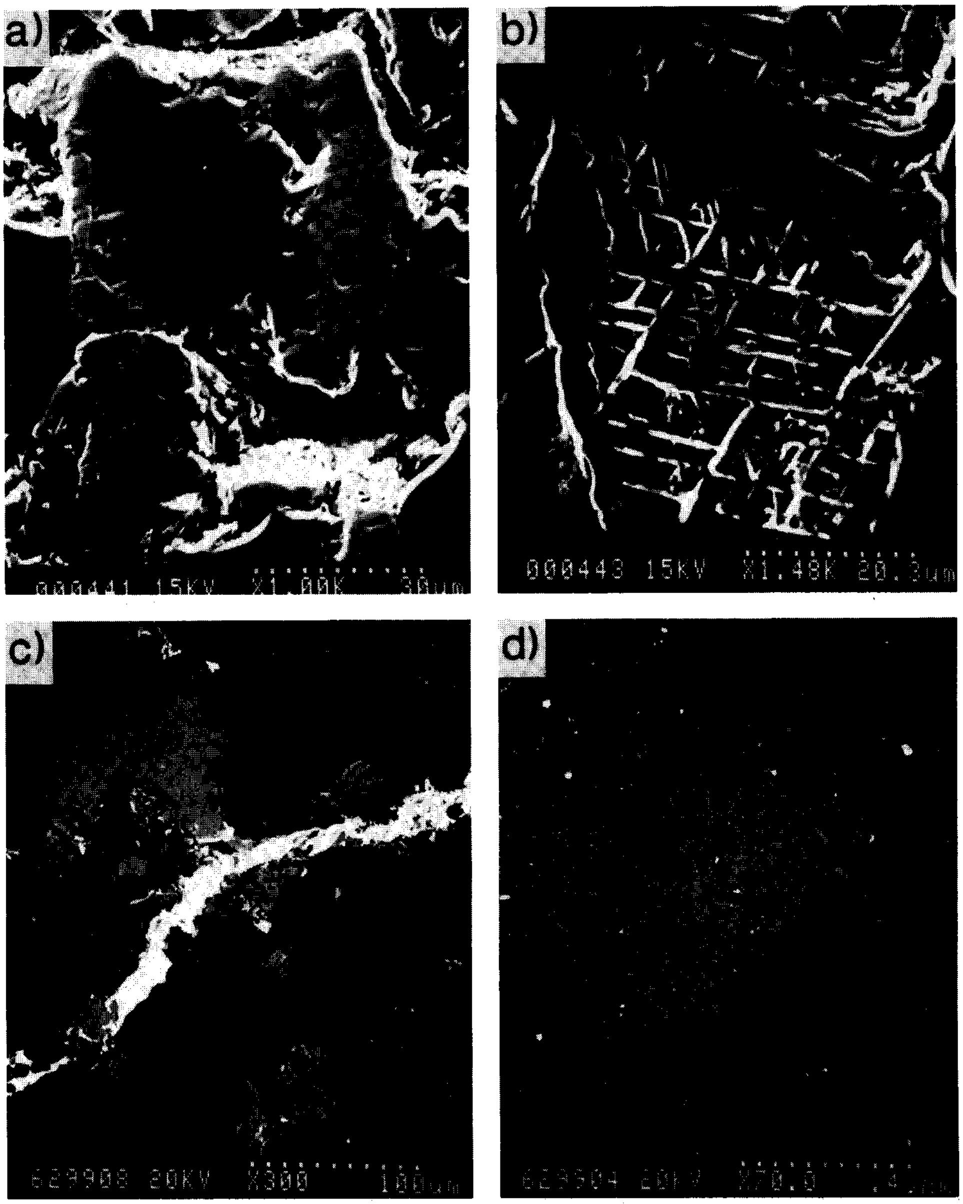

Fig. 7. Backscattered electron images of Fe-Ti oxides of selected samples. (*a* and *b*) Detrital grains from a heavy-mineral layer. (*a*) Rutile (dark gray) - hematite (light gray-intergrowth. (*b*) Martite with relict "trellis" lamellae. (*c*) Secondary (authigenic) hematite vein (white) cross-cut by a late calcite cement (light gray). This sample (site 2, Mesa Gallina) carries the steeply-up southerly direction interpreted as a late Mesozoic overprint. (*d*) Silt clasts from a microconglomerate in the Chinle Formation. The matrix is a calcite cemenet and is free of any form of hematite. The clasts contain abundant specularite (white) and pigmentary hematite.

specularite is the most common iron oxide (Figure 7). Generally, specularite grain size ranges between 1 and 50 m. Hematite is also abundant as microcrystalline pigmentary coating of quartz grains, large (e.g.,>10 m) replacements of magnetite (martite), pore filling cement, and grain overgrowths. Specularite occurs as small authigenic and variably sized detrital grains. Large authigenic specularite grains are relatively abundant only in red bed sites which carry the southerly and steep upwards magnetization (Figure 7c). Specularite is relatively scarce in sites carrying a large easterly and steep to moderate down component. Moreover, pigmentary hematite coating is quite irregular in these samples. On the other hand samples with univectorial demagnetization diagrams (e.g., Figure 4*a*), carrying the characteristic magnetization, are typically characterized by finer grains of specularite, relatively more abundant pigmentary hematite, and the absence of large grain overgrowths. The relatively high laboratory unblocking temperatures of the magnetization indicate that specularite, rather than pigmentary hematite, is the main carrier of the characteristic magnetization [*Collinson*, 1974; *Turner*, 1981].

INTERPRETATION OF DIRECTIONS

The direction of the magnetization of each individual component was determined using principal component analysis [*Kirschvink*, 1980]. End point directions were calculated for specimens that gave three or more points defining a linear segment in demagnetization diagrams. Great circle orientations

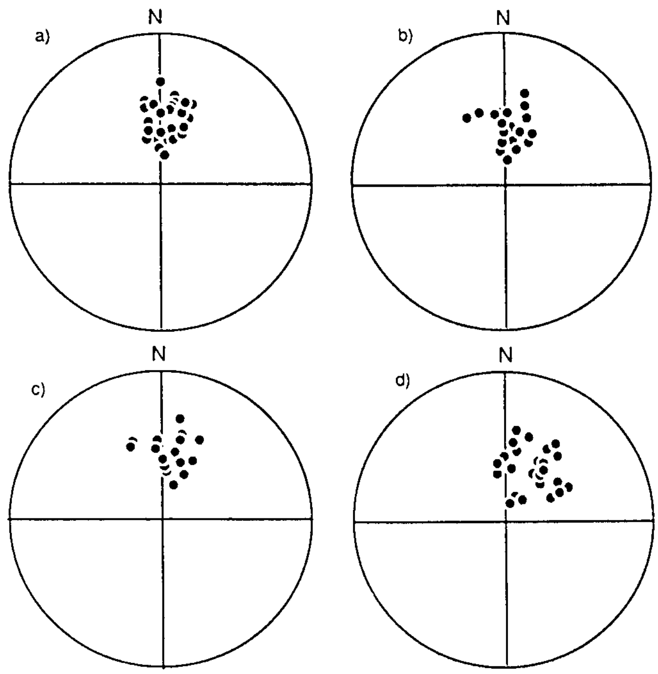

Fig. 8. Equal-area projections of sample directions (lower hemisphere) of the component interpreted as a secondary magnetization aligned with the present dipole field (I=54°). (*a*) in situ, (*b*) Carizo Arroyo, (*c*) Sevilleta, (*d*) Tejon. Directions are plotted in field coordinates and fail a fold test.

were calculated to estimate the characteristic magnetization direction in samples that did not yield a sufficient number of points to fit an origin-anchored line by *Kirschvink's* [1980] method. Only samples with maximum angular deviation values smaller than 10° were included in the site mean calculations. Site means that required combination of great circle and stable end point data were calculated using the method described by *Bailey and Halls* [1984].

Secondary Components

The northerly and downward directions from each locality are plotted on equal area stereographic projections in Figure 8, all in field coordinates. The directions are well clustered and clearly fail the fold test. Except for the Tejon result, the calculated means are statistically indistinguishable from the expected recent dipole field (RDF) direction. Directions from Tejon (mean: D=33.4°, I=57°) plot significantly east of both the expected dipole (I=54°) and the present day field direction (D=12°, I=63°).

The southeasterly and intermediate upward directions, combined for all four localities, are plotted in Figure 9, both in field coordinates and referred to the paleohorizontal. Dispersion decreases significantly after simple tilt correction (Table 1; Figure 9*b*) indicating that magnetization predates folding. However, the mean declination from Tejon samples again differs from the other localities by about 33°. The maximum precision parameter (k) of all four localities is obtained at 68% unfolding. A discordancy test was applied to the data according to *Fisher et al.* [1981]. The statistic En increases after tilt correction indicating a greater distance between the overall mean and the outlier direction (Tejon). The probability for the En statistic to be greater than observed (Table 1), is relatively small (0.206); thus, the test indicates that the Tejon direction is discordant. When only the remaining three locality directions are averaged maximum k is observed at 90% unfolding, but the difference between 90% and 100% unfolding is not significant. This suggests that the magnetization should not necessarily be considered as synfolding. The tilt in all cases was acquired during the rift formation in the late Cenozoic. If the intermediate upward and southerly directions from Tejon as well as the other localities are contemporaneous, then these data indicate that the Tejon locality has experienced a clockwise rotation of about 33.4° (+/-13.2°) relative to the other localities (the rotation error was calculated after Demarest [1983]).

A similar discrepancy (about 30°) was observed between the (low temperature) northerly and downwards component at Tejon and the remaining localities, thus suggesting that this magnetization component (carried in part by goethite) predates the rotation. In this case, however, the direction is defined by fewer points in the demagnetization diagram and the same effect may result from contamination by the easterly overprint; moreover, this component fails a fold test and there is no independent evidence that the rotation postdates the folding.

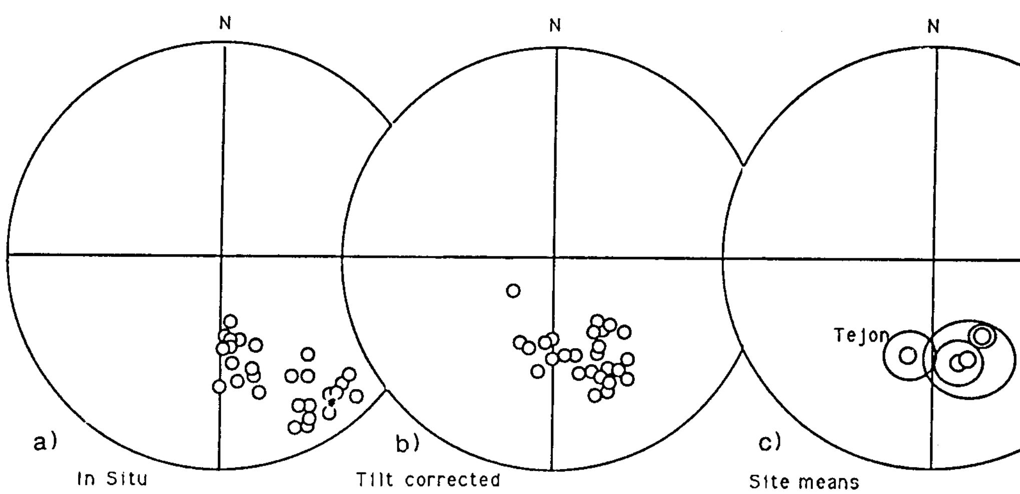

Fig. 9. Equal-area projections of sample directions (upper hemisphere) of the component interpreted as a late Mesozoic overprint: (*a*) in situ, (*b*) tilt corrected, (*c*) tilt corrected site means. Directions from Tejon are at variance with results from all other localities.

TABLE 1. Paleomagnetic Data and Associated Statistics: Permian Strata and Late Cretaceous/Early Tertiary (?) Overprint, New Mexico

Locality	N	In Situ D/I		Tilt Corrected D/I		k/α_{95}	Exp. Dir.
Permian Sevilleta Grant							
p1	7	156.9/+ 7.7		157.0/-10.5		66.6/ 7.4	
p2	4	157.4/+10.5		157.3/- 7.7		32.3/16.4	
p3	6	160.2/+16.2		158.2/- 0.4		45.4/10.1	
Mean	3			157.5/- 6.2		238.3/8	149.7-13.7
Locality	N	In Situ D/I		Tilt Corrected D/I		k/α_{95}	(a/b)
Late Cretaceous/Early Tertiary (?)							
1. Mesa Gallina	9	171.2/-53.5		146.9/-52.4		120.1/ 4.7	11.3/7.0
2. Sevilleta Grant	17	152.9/-31.7		163.2/-45.8		23.4/ 9.1	
3. Carizo Arroyo	3	131.4/-28.5		156.7/-45.7		67.8/15.1	
4. Tejon	9	139.0/-18.7		190.2/-50.2		64.4/ 9.4	
Locality	N	In Situ D/I	In Situ k/α_{95}	Tilt Correction D/I	Tilt Correction k/α_{95}	k_2/k_1	Discordancy En i.s./En t.c.
Overall mean (a) Late Cretaceous/Early Tertiary (?)	4	146.7/-33.6	16.5/23.2	164.8/-50.2	45.1/13.8	2.733	0.924/6.810
(max k=106, 68% un.)		149.4/-38.9	16.1/-23.8	156.8/-49.1	135.5/10.6	8.416	p[En>6.8]=0.2
Mean 1, 2, 3, (b)	3	max k=150, 90% un.					
	Poles:	Late Cretaceous/Early Tertiary (?)		70.3N-155.2E (b)			
		Permian		52.5N-112.2E			

D/I, declination/inclination; *k*, precision parameter; $\alpha95 = 95\%$ cone of confidence; *N*, number of samples. The En statistics have been calculated according to *Fisher et al.* [1981]. The En value increases significantly after tilt correction, which indicates a greater significance for the discrepancy between Tejon and the other localities. (a/b) is the angle (great circle) between the observed direction and the mean (a or b). Exp. Dir., expected Early Permian direction using the cratonic reference paleopole.

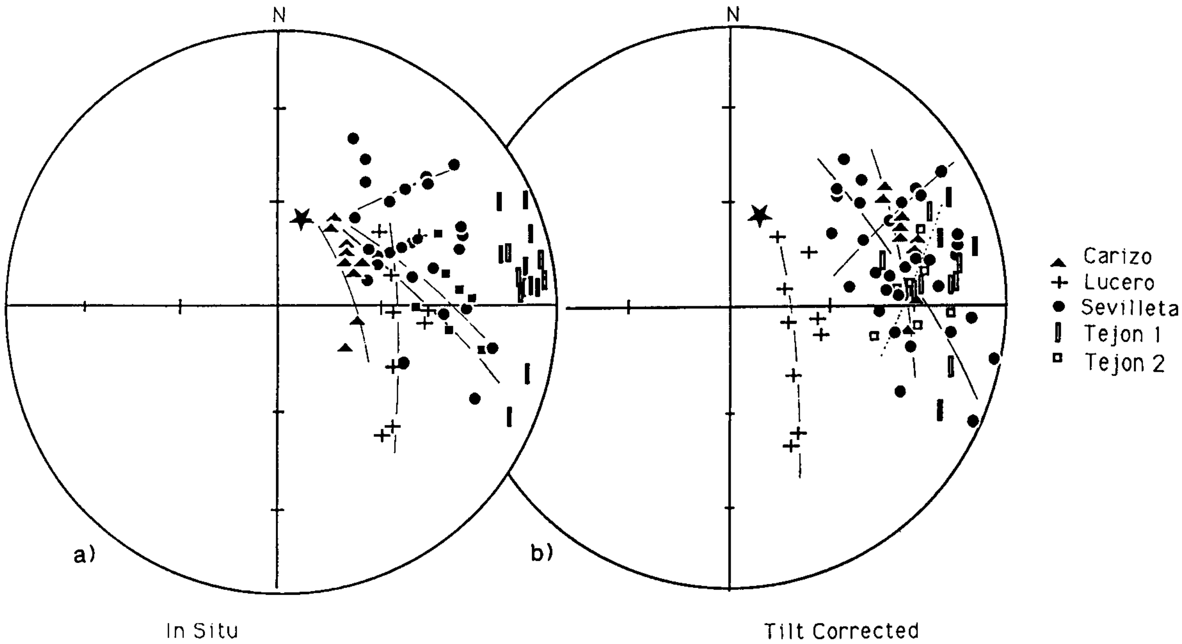

Fig. 10. Equal-area projections of sample directions of the easterly component interpreted as a composite (recent plus ancient) magnetization: (*a*) in situ, (*b*) tilt corrected. Open (solid) symbols project in the upper (lower) hemisphere. At Tejon, two sets of samples with different structural corrections are plotted. All samples from Lucero are of positive inclination. A few great circle lines have been drawn to illustrate the streaked distribution of directions at some localities.

The observation of approximately 33° of clockwise rotation along the southeastern margin of the Hagan Basin is consistent with the inferred sense of motion along the Tijeras and San Francisco faults (Figure 1). At present our data do not allow us to evaluate the areal extent of the rotated region. We note that *Brown and Golombek* [1985] have reported clockwise rotations on the basis of paleomagnetic data from late Cenozoic igneous rocks in the Jemez Block, a few tens of kilometers northwest of our sampling area. The mean calculated for the southeast and upwards component (using only the three "unrotated" localities, Table 1) indicates a paleopole located at 69.9°N-156.5°E. This pole plots near the late Mesozoic segment of North American APWP. This component is thus interpreted as a pre-tilting CRM, possibly of Cretaceous age, perhaps associated with the Laramide orogeny. Similar directions have been observed by *Jackson and Van der Voo* [1986] as remagnetizations in the Ordovician El Paso and Montoya formations in south central New Mexico.

Intermediate or otherwise abnormal directions have been previously observed in the Moenkopi by various authors. Based on the observation that intermediate directions occur at the same stratigraphic level as polarity transitions, they have been interpreted as records of transitional field configurations by *Shive et al.* [1984] and *Herrero-Bervera and Helsley* [1983]. Other studies have rendered intermediate directions as abnormal geomagnetic field configurations (excursions?) [*Helsley*, 1969; *Helsley and Steiner*, 1974]. Such interpretations require a very rapid magnetization acquisition over a span of a few hundred years. On the other hand, *Larson and Walker* [1982] argue that intermediate directions may be the result of mixing nearly antipodal normal and reverse components of magnetization. The composite of a large number of samples where mixing occurs in various proportions thus results in directions distributed along a great circle between the end points. This interpretation implies a slow magnetization acquisition over a span of up to several million years.

Intermediate, easterly, directions calculated by principal component analysis from free linear segments in demagnetization diagrams are plotted in Figure 10, both in situ and tilt corrected. Sample directions appear to form a set of streaks, with each streak defined by those samples with approximately the same structural correction. This may indicate that intermediate directions result from mixing of two magnetization components. Directions are slightly more scattered after tilt correction. In situ, some of the streaks trend towards the present-day field direction. Upon structural correction, however, the streaks change in such a way that the planes intersect near the Triassic characteristic direction. It appears then, that one of the "mixed" components postdates while the other predates tilting. This interpretation is, however, simplistic, because data from Sevilleta Grant and Tejon show a more complex trend. Directions from those areas appear streaked towards the Cretaceous (?) overprint. We have interpreted the easterly and intermediate directions as composite directions resulting from mixing of both ancient and relatively recent (RDF) diagenetic components. Such late diagenetic components, however, are generally carried by a fraction of magnetic phases with lower laboratory unblocking temperatures and might be viscous in origin.

Characteristic Magnetization

Site means calculated for the characteristic, Triassic, magnetization are plotted in Figure 11, for all four localities. Only the section sampled at Sevilleta Grant includes data from both the Moenkopi and Chinle formations. Paleomagnetic directions from the Tejon section show north-northeasterly declinations, which we believe reflect the clockwise rotation of this area, as suggested by the direction of the recent and Cretaceous (?) overprints as well.

A reversal test was applied to the data. The Chinle Formation data pass the reversal test, yet, only two sites have a reverse magnetization and the critical angle at which the null hypothesis

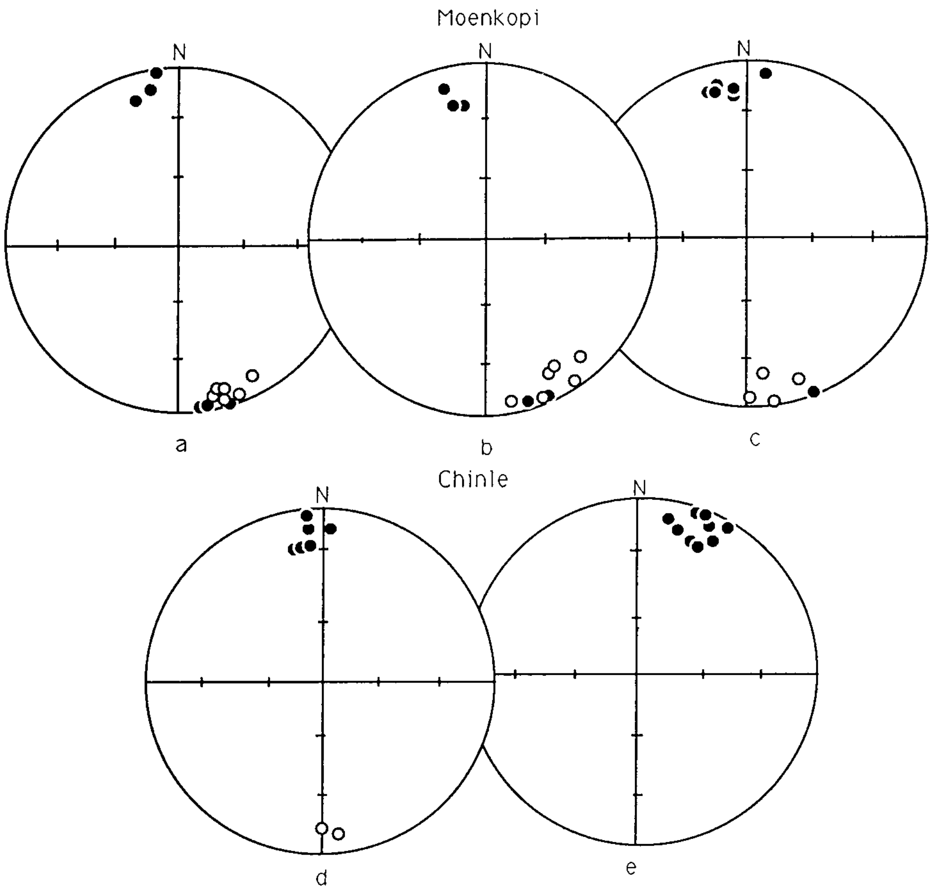

Fig. 11. Equal-area projections of the site means for the characteristic magnetization. Open (solid) symbols project in the upper (lower) hemisphere. Moenkopi Formation: (*a*) Mesa Gallina, (*b*) Carizo Arroyo, (*c*) Sevileta Grant. Chinle Formation: (*d*) Sevileta Grant and (*e*) Tejon. All directions have been corrected for simple tilt.

would be rejected is 11° [*McFadden and McElhinny*, 1990]. The Moenkopi results fail the reversal test at the 99% confidence level. The angle between the normal and (inverted) reverse mean is 9.8°. This suggests that the magnetizations in the Moenkopi are slightly contaminated with another component which systematically flattens the reverse directions (and/or steepens the normal polarity directions). A comparison between our overall mean and the results from Mesa Gallina locality alone (where the reversal test passes; see Table 2) shows that the magnitude of the contaminating effect is likely to be as small as 3° (an effect in paleopole location of no more than 1.5°). Thus, the effects of the contamination, when averaged, are insignificant.

Conglomerates in the Moenkopi and Chinle formations are common; in the sections sampled the majority are intraformational pebble-size conglomerates of rounded sandstone and siltstone clasts or rip-up siltstone clast conglomerates. Maximum clast dimensions range between 0.1 and about 1.5 cm. We sampled conglomeratic beds at three localities. In the laboratory, specimens of individual clasts were prepared according to the microanalysis technique described by *Geissman et al.* [1988]. Microspecimen magnetizations were measured in a 2G Enterprises cryogenic magnetometer at the University of New Mexico paleomagnetic laboratory. Specimens were thermally demagnetized in eight steps up to 630°C. Typical demagnetization diagrams are shown in Figure 12. Demagnetization behavior is relatively noisy, it is characterized by the removal of two components: a low temperature component sometimes parallel to the present day field and a higher unblocking temperature component. The directions isolated are randomly distributed (Figure 12a), therefore the conglomerate test is positive, which implies that the characteristic magnetization was acquired rapidly after deposition and before disaggregation. Microconglomerate silt clasts have roughly the same petrological characteristics as siltstone beds (abundant hematite replacing magnetite, pigmentary hematite, and detrital ilmenite-hematite intergrowths). The matrix, in most cases, is a calcite cement characterized by the absence of either pigmentary hematite or specularite (Figure 7). Specularite in the matrix was observed only when the matrix is made of sand grains. These observations indicate an early formation of the hematite in the silt clasts. The characteristic magnetization is thus interpreted as an "early" CRM and/or a DRM acquired during or soon after deposition.

Virtual geomagnetic poles (VGP) were calculated from each individual site. VGP distributions are shown in Figure 13. Distributions are slightly elliptical (Tables 2 and 3). This phenomenon is clearly more evident in the Moenkopi distribution (Figure 13*a*). Such elliptical distribution is not atypical of paleomagnetic data. The long axis of the ellipse of the VGP distribution in the Moenkopi Formation trends more or less east-west. The mean calculated from such a grouping is the same whether or not a Fisherian distribution is assumed. Because of the orientation of the long axis, the magnetizations of the Moenkopi Formation do not appear to be affected by a systematic overprinting in the RDF direction. Instead, a small amount of polar wander, or relatively minor contamination with

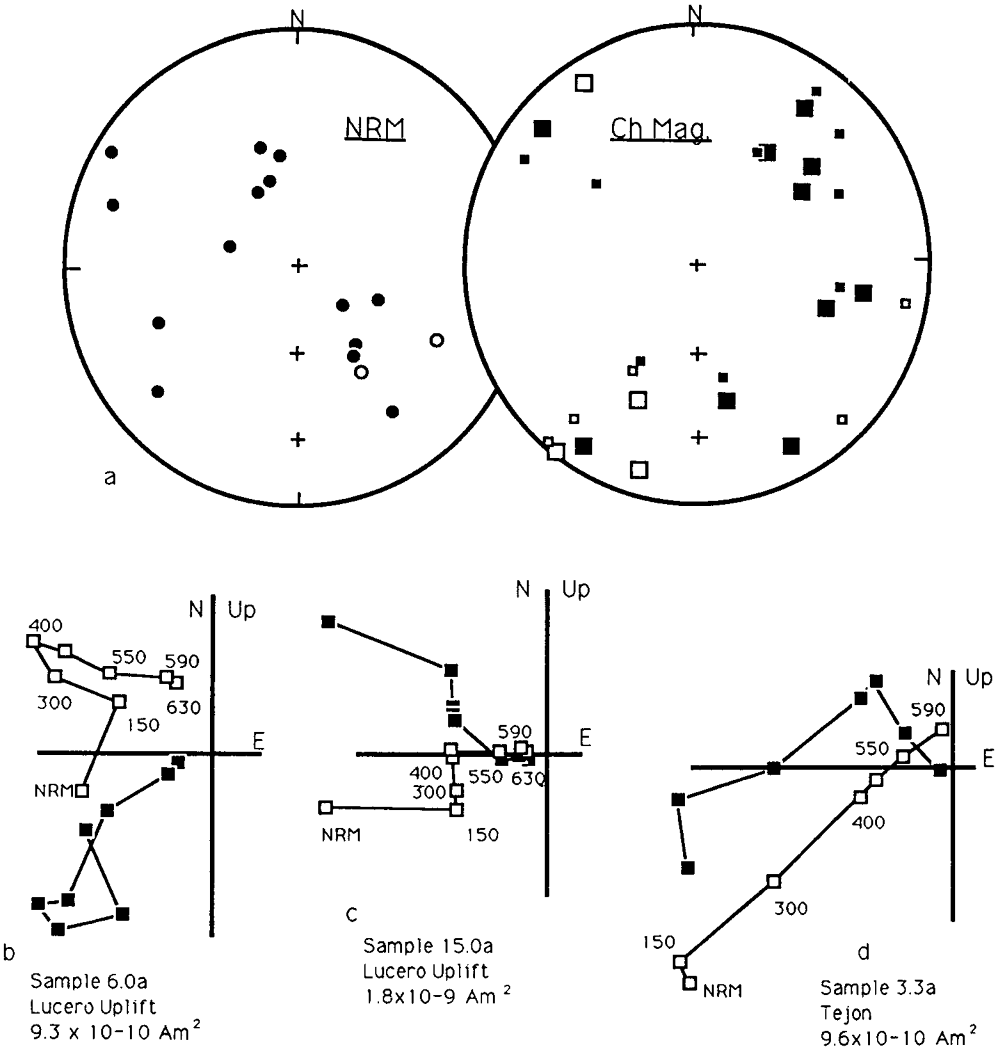

Fig. 12. Paleomagnetic results from a microconglomerate test involving progressive thermal demagnetization of 16 oriented hematitic siltstone/mudstone clasts conglomerate beds in the Moenkopi and Chinle Formations. (*a*) Equal-area projection showing NRM directions (circles, in situ) and directions of magnetization components isolated in demagnetization (small squares, uncorrected, and large squares, corrected for "bedding"). Two of the 16 clasts did not yield definable magnetizations in thermal demagnetization; hence only 14 magnetization directions are plotted. (*b-d*) Orthogonal demagnetization diagrams for three selected hematitic clasts from three samples, shown in insitu coordinates. The NRM moment for each clast is given below the sample identification. Symbols in demagnetization diagrams are as in Figure 4.

a Late Triassic magnetization may produce the distribution observed. We have noticed that the paleopole obtained for the normal (generally older) directions lies to the west of the pole determined for the reverse (younger) directions. That is in the opposite sense to the northwesterly trend of the APWP. This result suggests that the pole back-tracked before heading westwards in the Late Triassic.

Site means for the Late Permian red beds sampled at Sevilleta Grant are presented in Table 1. Paleomagnetic directions are well grouped at both the site and formation level. These data represent a stratigraphic interval of about 5m. No field tests were possible to constrain the age of this magnetization. Nonetheless, the Permian magnetizations are consistently more southeasterly than the Triassic directions and we have interpreted those directions as Permian in age. Permian carbonates sampled at other localities did not yield reliable magnetizations.

DISCUSSION

Triassic APWP

Paleomagnetic data and associated statistical parameters are summarized in Tables 2 and 3 for the Moenkopi and Chinle formations, respectively. The paleopole for the Moenkopi Formation lies at 57.6°N-100.3°E (N=36 sites; K=74.1; A_{95}=2.8°). The paleopole for the Shinarump and the Bluewater Creek (unnamed) members of the Chinle Formation lies at 60.8°N-88.9°E (N=17 sites; K=130.3; A_{95}=3.1°). Paleopoles are compared with other poles from stable North America in Figure 14.

During Triassic time paleomagnetic poles "tracked" in a west-northwest direction from a position at about 48°N-115°E (Chugwater Formation, Red Peak Member, WY; *Shive et al.* [1984]) in the earliest Triassic to a position at about 60°N-65°E (Wingate Formation, UT, *Reeve* [1975]; Moenave Formation,

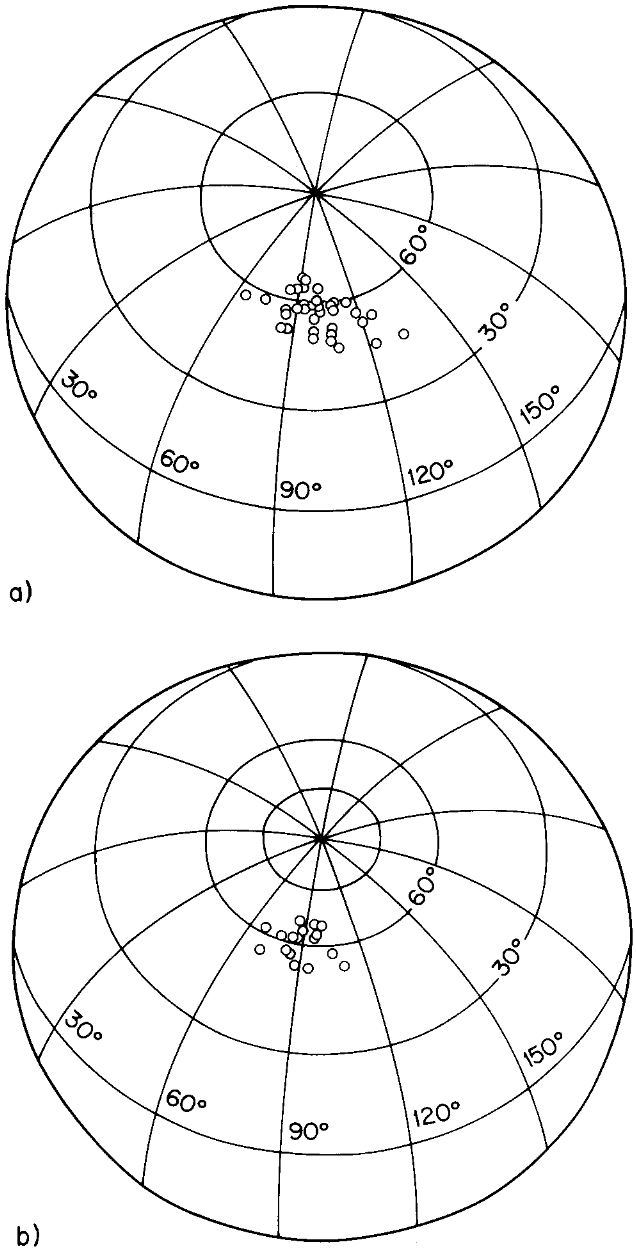

Fig. 13. Orthographic projection of virtual geomagnetic poles calculated from the site means. (*a*) Moenkopi Formation and (*b*) Chinle Formation.

AZ, *Ekstrand and Butler,* [1989], *Clark and Fastovsky* [1986]) in the earliest Jurassic (Figure 14). The paleomagnetic Euler pole (PEP) method suggested by *Gordon et al.* [1984] uses a small circle to describe the APWP from the Carboniferous to the latest Triassic. This method evaluates the hypothesis that the plate motion direction with respect to the rotation axis during that time was constant. According to this model, paleopole determinations should be located within a small circle band of reasonable width determined by small random perturbations. Applying this methodology to the entire Carboniferous to latest Triassic segment of the APWP is problematic because mid-Triassic poles from the Abbot and Agamenticus plutons in Maine [*Fang and Van der Voo*, 1988] and the Fundy Group in Nova Scotia [*Symons et al.*, 1989], and Late Permian poles from New Mexico, Oklahoma, and west Texas [*Peterson and Nairn*, 1971; *Molina-Garza et al.*, 1989] fall significantly off the PEP small-circle path of *Gordon et al* [1984]. Moreover, key poles in the PEP analysis of Gordon et al. are out of spatiotemporal sequence. For instance, the "N1" pole of *Smith and Noltimier* [1979] is Hettangian in age and lies east of the Sinemurian-Pliensbachian Wingate and Moenave poles, in the eastbound J1-J2 track of *May and Butler* [1986]. A recent revision of the paleomagnetism of the Hettangian zone in the Newark Basin [*Witte and Kent*, 1990] suggests that such discrepancy may be caused by insufficient removal of a secondary overprint. However, the Hettangian pole of Witte and Kent is also out of spatiotemporal sequence since it lies east of the Norian age poles of the upper strata of the Chinle Formation in the Tr-J PEP track of *Gordon et al.* [1984].

Debate about the shape of the Triassic segment of the APWP is a reflection of, primarily, discrepancies between paleomagnetic poles from the supposedly time-equivalent Newark Series, and the Chinle Formation and related strata [*Witte and Kent*, 1989, 1990], and problems in the time calibration of the path because of the difficulties in correlation among (and dating of) continental red beds. The debate is further complicated by the uncertainty about the amount of tectonic rotation of the Colorado Plateau, which may cause a systematic deviation of the paleomagnetic poles from that area.

The pole for the Moenkopi of central New Mexico is statistically indistinguishable from other Moenkopi poles of the Colorado Plateau [*Helsley and Steiner,* 1974; *Elston and Purucker,* 1979; *Baag and Helsley,* 1974]. The Shinarump/Bluewater Creek (Carnian) members of the Chinle yield a pole indistinguishable from the (Norian) Bull Canyon Formation (Upper Shale member) of eastern New Mexico off the plateau [*Bazard and Butler,* 1989]. The Shinarump/Bluewater Creek member pole is slightly west (e.g., 7°-13°) of other (cratonic) Carnian poles such as those from the Popo Agie [*Van der Voo and Grubbs*, 1977], the Newark Basin lower beds [*Witte and Kent,* 1989], and plutons from Maine [*Fang and Van der Voo,* 1988].

The main effect of the hypothesized clockwise rotation of the Colorado Plateau is to have translated paleopoles westwards by about 10° in longitude. The rotation of the Colorado Plateau is supported by the observation of systematic deviations in that direction of poles from this area. However, accurate evaluation of the amount of rotation is difficult because of the relatively small amplitude of the discrepancy, the relatively small high-quality paleomagnetic database, and the relatively poor age determination of most high-quality paleopoles. For that reason, tests for rotation of the plateau are positive but statistically insignificant [*Bryan and Gordon,* 1988].

Assuming that the stratigraphic correlations suggested in this paper are correct, a small clockwise rotation of the sampling localities in central New Mexico is required to bring the Triassic paleopoles from this area into agreement with the cratonic data; such a rotation is similar to that proposed for the Colorado Plateau. Ignoring the Tejon results for a moment, we question whether the observed declination deviations are a local effect due to rotation about the vertical at the sampling sites, because samples were collected at relatively widely spaced localities along both sides of the rift. Moreover, between localities (1, 2 and 4 in Figure 1) variations of the declination for the Triassic and the Cretaceous (?) components are not systematic. The stratigraphic sections sampled in central New Mexico are located at the eastern margin of the Colorado Plateau within a tectonically disturbed zone of the craton. What

TABLE 2. Paleomagnetic Data and Associated Statistics: Moenkopi Formation, New Mexico

Site	N/n	In Situ D/I	Tilt Corrected D/I	k/α_{95}	VGP Lat. N	VGP Long. E
Mesa Gallina (34.6N-107.1W)						
c2-c3	7/5	353.3/ +0.8	353.0/ +2.7	46/11.4	56	85.3
c4	4/2	352.9/ +8.4	349.8/+11.3	- / -	59.5	93.3
c5	6/5	171.6/ -6.2	169.2/ -8.9	54.4/10.5	58.1	93.8
c6	7/4*	169.5/ +7.0	171.2/ +4.4	26.8/36.7	52.2	87.3
c7	12/10*	161.9/ -5.2	160.3/ -4.9	39.7/ 9.1	52.9	106.8
c8	7/5*	167.4/ -4.2	165.8/ -5.7	45.1/11.5	55.5	98.5
c9	4/2*	348.4/+16.8	342.8/+17.9	28.5/33.6	60	108.6
c10	8/6*	171.0/-11.0	167.4/-12.9	23.9/20.6	59.5	98.2
c12-13	9/9*	164.2/ +1.5	164.6/ +0.7	26.3/11.7	52.1	98.5
c14	7/7*	170.8/ +7.9	172.8/ +4.9	163.8/ 6.0	52.2	84.7
c15-16	9/6*	169.0/-10.7	165.4/-12.2	26.8/19.5	58.4	101.5
c17	3/3	157.8/-15.1	153.3/-13.1	61.5/15.9	52.9	120
Normal	3		348.6/+10.7			
Reverse	9		165.6/ -5.3			
Mean	12	348.2/ 6.8 k=103; α_{95}=4.3	346.3/ +6.8 k=79; α_{95}=4.9		56.2	98.1
Sevilleta Grant (34.2N-106.7W)						
mk13	6/6*	345.2/+ 3.7	347.9/+14.2	42/19.6	60.6	99.7
mk12	5/4	4.8/+ 1.0	5.1/ +3.4	21.5/20.3	57.1	63.9
mk11	7/7	344.6/+ 1.7	346.1/+11.0	138.1/5.2	58.6	100.6
mk8	4/4	347.3/+ 6.7	351.6/+18.0	93.5/9.6	63.9	92.4
mk7	8/5	352.0/+ 5.8	354.7/+15.0	47.5/11.2	63	85
mk6	5/5	161.2/+ 4.0	162.3/-12.5	95.4/7.9	57.7	107.7
mk5†	7/5	169.8/- 3.4	173.0/-16.9	37.8/12.6	63.6	89
s2	8/7	341.9/- 1.1	343.4/+14.6	58.3/8	59.1	107
s3	5/5	348.5/- 1.5	350.6/+16.0	347.1/4.1	66.7	91.1
s4	5/5	338.9/+ 3.6	340.0/+18.7	124.9/6.9	59.3	114.6
s5	5/5	173.8/+ 4.2	173.7/ -3.9	43.5/11.7	57.2	85.1
s6†	7/4*	178.9/- 0.6	179.8/ -5.5	12.5/36.4	58.4	73.7
s7	4/3	162.8/+15.8	159.6/ +3.2	341.2/6.7	49.4	105.6
Normal	8		350.0/+14.0			
Reverse	5		169.7/ -7.2			
Mean	13	348.4/+ 0.5 k=74; α_{95}=4.8	349.9/+11.4 k=64; α_{95}=5.2		60.4	93.8

Carizo Arroyo (34.7N-107.1W)						
ca3-4	7/12	336.2/+15.6	346.7/+20.3	32.7/10.7	63.9	100.5
ca5	4/4	338.1/+18.9	352.2/+22.7	36.1/15.5	66.2	92.6
ca6	5/5	340.9/ 6.0	346.3/+10.8	177.8/ 5.8	58.2	100
ca7	4/8	145.1/ -3.9	151.9/-18.1	75.1/10.7	53.9	124.8
ca8	7/8	149.3/ -4.2	155.6/-16.0	113.2/ 5.7	55.6	118.3
ca9	6/6	139.2/ 4.8	144.2/-14.4	94.9/ 6.9	45.6	133.6
ca10	8/8	161.0/ 5.6	161.8/ -0.5	24.8/12.4	51.1	105.9
ca11-12	5/11	166.7/ -6.3	171.2/ -7.7	20.4/17.3	58.3	90.1
ca13	5/6	149.0/ +8.8	148.0/ -5.4	87.3/ 8.2	46.2	122.8
ca15	5/5	162.5/+11.4	157.5/ +4.3	77.8/ 8.7	47.5	108.2
ca16	5/6	167.5/ +7.3	163.9/ +3.9	113.17/ 7.2	50.4	98.5
Normal	3		348.3/+18.0			
Reverse	8		156.8/ -6.8			
Mean	11	336.0/ +1.5	339.6/+10.0		55.6	107.1
		k=36; α_{95}=7.7	k=36; α_{95}=7.7			

Overall	N/n	In Situ D/I	Directions	k/α_{95}	Poles	
Fold Test		344.2/+2.9	345.3/ +9.4			
(3 localities)		k=106.4	k=204.9			
Bingham stat.						
Max. eigenvector			346.4/+10.1		57.6	100.3
			$k1$=28.3/$k2$=-24.8		$k1$=-103.2/$k2$=-24.5	
Test for circ. sym.						
Oval Azimuth			105.4		111	
Bipolar			0.16		22.6	
Girdle			419.97		419.9	
Normal	14		349.3/+14.1		60.9	95.3
Reverse	22		163.4/ -6.3	$p[x>9.8]=.002$	55.1	102.9
Overall	36		346.4/+10.1	74.1/ 2.8	57.6	100.3

N/n, samples demagnetized/samples used for site mean calculation; D/I, declination/inclination;
VGP, virtual geomagnetic poles.
*Sites where great circle and stable end points were combined to calculate site mean.
†Sites where mixed polarities were observed.

TABLE 3. Paleomagnetic Data and Associated Statistics: Chinle Formation, New Mexico

Site	N/n	In Situ D/I	Tilt Corrected D/I	k/α95	VGP Lat.N	VGP Long.E
Sevilleta Grant (34.2N-106.7W)						
mk4	3/3	175.4/-6.3	179.5/-17.9	60.5/16	63.2	96.8
mk3	4/4	344.6/ 8.5	349.3/ 23.3	20.8/20.6	65.6	99.6
mk1-2	6/5	171.6/ 0.0	173.6/ 13.1	10.2/22.1	61.8	86.6
s7a-s8	3/8	(169.3/-7.0)	(172.9/-13.9)	8.2/46.2	61.9	88.2
s9	6/5	354.9/ 3.8	355.1/ 4.9	24.5/15.8	57.9	82.5
s10	6/5	0.0/-1.8	2.6/12	129.3/6.8	61.7	67.7
s11	6/5	354.5/-1.1	354.9/12.5	239.3/5.0	61.7	83.9
s12	6/4	354.8/24.9	355 /21.9	107.5/8.9	66.7	85.8
s13	6/5	346.1/ 8.9	351.1/22.3	62.7/9.7	66	95.3
Normal	6		354.8/+16.2			
Reverse	2		176.6/-15.5	p[x>1.9]=0.9		
Mean	8	352.7/ 6.2 k=66; α95=6.9	355.2/16.0 k=113;α95=5.2		63.4	86.8
Tejon (35.3N-106.4W)						
t1	6/4	12.1/31.9	25.6/19.4	64.7/11.5	64	88.2
t2	7/5	9.0 /29.1	21.7/18.4	39.3/12.4	62.5	96.1
t3	6/4	28.9/15.7	32/2	54.5/12.6	55.6	70.1
t4	10/7	20.2/19.5	23.9/0.9	64.2/9.2	54.3	87.6
t5	7/6	14.4/21.4	20.3/1.8	86.7/7.2	53.9	93.8
t6	4/4	10.6/21.0	26.1/5.8	59.3/12.0	57.1	84.6
t7	4/4	18.4/34.8	30.0/13.1	32.2/16.4	61.3	77.8
t8	6/4	352.2/16/2	11.7/9.7	68.6/11.2	54.3	109.9
t10	6/4	7.6 /21.4	15.7/13.9	15.7/24.6	58	105.4
Mean	9	12.6/23.8 k=71; α95=6.1	23.0/9.5 k=71;α95=6.1	*	58.5	90.5

Overall			Directions		Pole	
Bingham stat.			352.6/+12.7 k1=34.8/k2=24.4		60.3 k1=-75.7/k2=-31.6	88.7
	Test for circ. sym.	oval azimuth=	166.6		102.4	
		bipolar=	0.56		3.52	
		girdle=	195.35		258.1	
Overall	17		352.6/+12.7	130.3/3.1	60.8	88.9

N/n, samples demagnetized/used in mean calculation; *D/I*, declination/inclination; VGP, virtual geomagnetic poles
*VGP's from Tejon and overall Tejon mean were calculated applying a strike correction of 33° (counterclockwise) to the (unrotated) directions listed.
†Sites 7a and 8 were excluded from the calculations.

is not clear is the question of whether this area was rotating rigidly with the plateau, or whether it experienced a similar sense rotation via an independent deformation mechanism. At least a small component of rotation of the Colorado Plateau has been attributed to opening of the Rio Grande rift. The three sites in the Late Permian "Bernal Formation" red beds that underlie the section at Sevilleta Grant yielded a paleopole located at 52.5°N-112.2°E (D=157.5°, I=-6.2°, N=3 sites; k=238.3; alpha$_{95}$=8°), again located to the west of the cratonic reference pole (51.4°N-126.2°E [after *Molina-Garza et al.*, 1989]; Dec$_{obs}$-Dec$_{exp}$=7.6° +/-7.1°), which is consistent with the rotation suggested by the Triassic data. It is clear that portions of central New Mexico appear to have rotated as much as (and perhaps with) the Colorado Plateau.

The Early Permian Abo Formation of central New Mexico studied at Abo Pass, south of the Manzano uplift (Figure 1), yielded a paleopole at 49.7°N-118.3°E [*Steiner*, 1988], which at first glance appears to be in general agreement with other poles; the position of the Abo pole then would indicate that central New Mexico did not experience rotation. However, in the formation-mean pole calculation, *Steiner* [1988] omitted data from cross-bedded strata which provided a more westerly longitude for the formation pole. Moreover, results from *Peterson and Nairn* [1971] for the Abo Formation (pole at 46°N-116°E) are also located slightly west of other Early Permian reference results such as those for the upper part of the Casper Formation in Wyoming, which produced a paleopole at about 123.4°E [*Diehl and Shive*, 1981] and the Pictou Group of New Brunswick which produced a paleopole at about 125.5°E [*Symons*, 1990]. Interpretation of Permian paleomagnetic poles had been problematic because they did not appear to show significant rotation in contrast to older (Pennsylvanian) and younger (Triassic and Jurassic) data from the Colorado Plateau [*Steiner*, 1986, 1988]. Perhaps this discrepancy resulted from the choice of reference poles and the areas (including central New Mexico) for which they were determined, because there are few Early Permian results for cratonic areas outside the Colorado Plateau [*Symons*, 1990]. An Early Permian cratonic paleopole

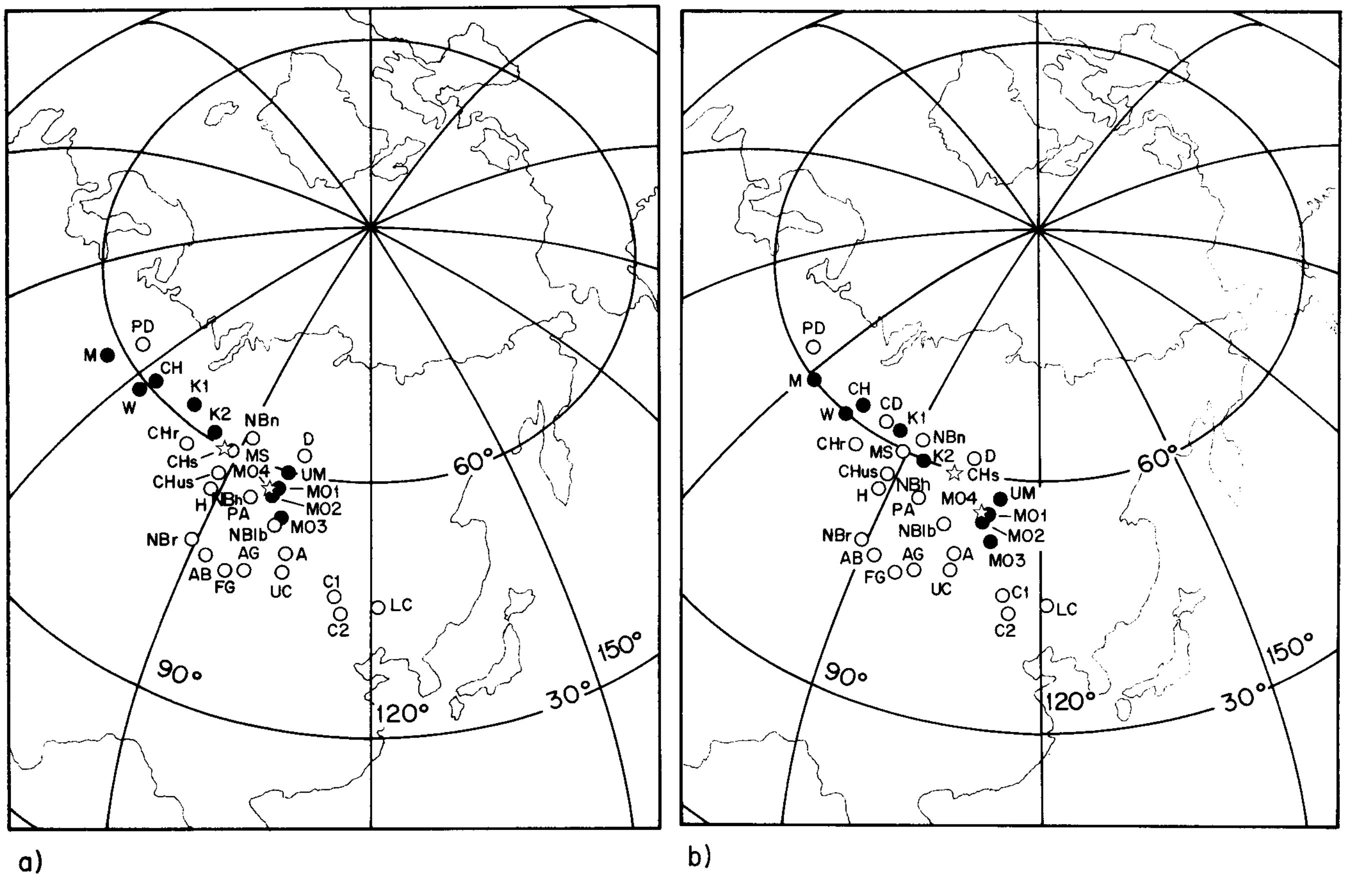

Fig. 14. Triassic data for stable North America. Data and pole symbols from Table 4. Solid symbols are from the Colorado Plateau. Stars refer to results from the present study. In Figure 14*b*, palepoles from the Colorado Plateau and central New Mexico have been corrected for a small clockwise rotation according to the parameters of *Bryan and Gordon* [1988] time scale.

position at slightly more easterly longitude (about 125°E) would be in better agreement with the well defined European Early Permian pole (at 46°N-125°E) rotated to North American coordinates by closing the Atlantic Ocean [*Van der Voo*, 1990]. In Figure 14*b* poles from the Colorado Plateau and central New Mexico have been replotted assuming a rotation of 5.4° according to *Bryan and Gordon* [1988]. Such a rotation diminishes the discrepancy between cratonic and plateau data.

Our results seem to favor the interpretation that tectonic rotations in central New Mexico are closely tied to rotation of the Colorado Plateau. However, more local scale deformation associated with middle to late Cenozoic formation of the Rio Grande rift and/or uplift mechanisms and oblique-slip faulting cannot be discounted [e.g., *Hayden and Mawer*, 1991]. Systematic deviations in all Early and Late Permian, as well as Middle and Late Triassic data from relatively widespread localities suggest the operation of a mechanism allowing for uniform-sense clockwise rotation within central New Mexico.

Triassic and earliest Jurassic paleomagnetic data for North America are summarized in Table 4. Results from central New Mexico and the Colorado Plateau have been corrected for clockwise rotation of 5.4° and temporal correlations have been indicated. Inspection of Table 4 suggests that discrepancies in the Triassic data described above are much less pronounced after correcting for rotation and assuming that the proposed stratigraphic correlations (e.g., Figure 3, Table 4) are correct. The corrected pole for the lowermost members of the Chinle Formation is located at 60°N-99°E. Preliminary results reported by *Bazard and Butler* [1989] for the Bull Canyon Formation (formerly upper shale member of the Chinle Formation, Figure 3) in eastern New Mexico indicate an Early Norian pole located at 57°N-88°E. The Redonda Formation [*Lucas et al.*, 1985] (formerly Redonda Member of the Chinle Formation) was studied in eastern New Mexico by *Reeve and Helsley* [1972]. The Redonda pole is located at 58°N-79°E. The Redonda Formation overlies the Bull Canyon Formation and is the youngest Triassic unit in the Tucumcari basin. The Redonda Formation has been assigned a middle to late Norian age. Based on litho-stratigraphic correlations as well as paleontologic data, deposition of the Shinarump (Agua Zarca) Member-Bull Canyon Formation-Redonda Formation sequence spanned late Carnian to late Norian times. Thus, the Shinarump-Bull Canyon-Redonda sequence documents a late Carnian to late Norian rapid apparent polar wander of about 12° (great circle distance) along a fairly uniform track. Upper Carnian-lower Norian results from the lower red beds of the Newark Supergroup (Lockatong and lower Passaic Formations) are at slightly more easterly longitudes than the track described by the Chinle results, yet the difference between the (Carnian) Chinle results and the Newark Supergroup is no longer statistically significant. Moreover, results for the Chinle Formation and related strata in eastern New Mexico are in good agreement with other Carnian and Norian results such as the Popo Agie (Wyoming) and the Manicouagan Structure (Quebec). Some discrepancy between paleomagnetic results from the upper Chinle (Redonda Formation in New Mexico, and Owl Rock

TABLE 4. Triassic and Earliest Jurassic Data From North America

Colorado Plateau	Lat.	Long.	k	α_{95}	Reference	Craton (NE N. America)	Lat.	Long.	k	α_{95}	Reference
L. Triassic-E. Jurassic											
Kayenta, UT	60	94	51	10	1 K1	Diabases, PA	62	105	118	2	11 D
Kayenta, UT	62	86	81	7	2 K2	Holyoke, MA	55	88	41	11	12 H
Moenava, AZ	60	62	45	5	3 M	Caraquet dike, N.Br.	62	82	-	-	13 OD
Wingate, UT	60	73	-	8	4 W	Newark, Hett., NJ	55	95	72	5	14 NBh
Norian Chinle, UT	62	75	892	4	4 CH	Newark, N, NJ, PA	62	91	8	3	15 NBh
						Neward, R, RJ, PA	49	89	50	5	15 NBr
Carnian						Newark, lowbeds, PA	54	102	50	5	16 NBlb
Chinle, lower beds, NM	60	99	130	3	5 CHs	Abbot pluton, ME	48	92	242	4	17 AB
						Agamenticus pl.,ME	48	99	258	3	17 AG
						Fundy Group, N.S.	45	97	21	7	18 PG
M. Triassic Upper Maroon, CO	58	112	26	9	6 LM						
Moenkopi, NM	56	109	74	3	5 MO4						
Moenkopi, AZ	56	110	10	2	7 MO1						
Upper Moenkopi, CO	53	111	102	3	8 MO3						
U. Moenkopi, drill, CO	55	109	368	6	9 MO2						
E. Triassic Lower Moenkopi, CO	55	107	85	5	10 MO						

1. *Johnson and Nairn* [1972]; 2. *Steiner and Helsley* [1975]; 3. *Ekstrand and Butler* [1989]; 4. *Reeve* [1975]; 5. this study; 6. *McMahon and Strangway* [1969]; 7. *Purucker et al.* [1980]; 8. *Helsley and Steiner* [1974]; 9. *Baag and Helsley* [1974]; 10. *Helsley* [1969]; 11. *Beck* [1972]; 12. *Irving and Banks* [1961]; 13. *Seguin et al.* [1981]; 14. *Witte and Kent* [1990]; 15. *McIntosh et al.* [1985]; 16. *Witt and Kent* [1989]; 17. *Fang and Van der Voo* [1988]; 18. *Symons* [1990]; 19. *Dooley and Smith* [1982]; 20. *Reeve and Helsley* [1972]; 21. *Irving et al.* [1976]; 22. *Bazard and Butler* [1989]; 23. *Van der Voo and Grubbs* [1977]; 24. *Grubbs and Van der Voo* [1976]; 25. *Shive et al.* [1984]; 26. *Herrero-Bervera and Helsley* [1983].

Pole symbols as in Figure 14. Paleomagnetic poles from the Colorado Plateau have been rotated according to *Bryan and Gordon* [1988].

Member in Utah) and the upper Newark Supergroup is still unresolved. Studies in the Newark Supergroup, which presumably was deposited in a time interval that spanned the Middle Carnian to the Early Jurassic, suggest a nearly stationary polar wander pattern from late Carnian to Norian and Hettangian times (from about 225 to 206 Ma), because results cluster bewteen 95°E and 102°E. Such an APW pattern implies a significantly higher rate of APW during the earliest Jurassic (about 3.4°-4.8°/m.y.), because the Hettangian pole lies at 95°E [*Witte and Kent*, 1990], while in the Sinemurian the pole lies at about 62°E (corrected after *Bryan and Gordon* [1988]). It may be argued that the resemblance of the Norian results from the Newark basin to the Hettangian data is at best suspicious. The recent recognition of significant Middle Jurassic overprinting in the Newark Supergroup [*Witte and Kent*, 1989, 1990] could suggest that demagnetization attempts to remove Jurassic-aged contributions to the NRM of the Norian strata of the Newark Basin may have been insufficient. Similarly, it can be argued that it is the upper Chinle strata which have been (partially) affected by Sinemurian aged remagnetizations, according to the CRM acquisition model of Larson et al. [1982]. A more rapid CRM acquisition in the Newark Basin would be promoted by more rapid and deeper burial of a thicker sedimentary column. However, more recent studies of the Chinle strata have confirmed the general reliability of previous Chinle results in the Colorado Plateau [*Bazard and Butler*, 1990]. Thus, we favor the APW sequence indicated by the Chinle strata. We believe that it is possible that the Newark Basin paleomagnetic directions may be affected by structural complexity, such as syn-depositional tectonic rotation and faulting [*Olsen and Schlische*, 1990; *Van Fossen et al.*, 1986] or insufficient removal of Mid-Jurassic, or younger, overprints [*McIntosh et al.*, 1985]; alternatively the APWP may have back-tracked temporarily during the Norian and Hettangian.

No data have been obtained which support polar wander to locations at lower latitudes (about 48°N) as suggested by data from the Maine plutons and Nova Scotia red beds. This discrepancy, still unresolved, could be partially explained if there is greater structural complexity in the northeastern United States than previously realized, as suggested, for example, by *Manning and de Boer* [1989], resulting in a slight tilt of the plutons.

Triassic Magnetostratigraphy

We have constructed a Triassic magnetostratigraphic sequence (Figure 15) based on the correlation of polarity sequences previously published, additional data obtained in the present study, and lithostratigraphic and biostratigraphic correlation of rocks in the southwestern United States, mostly from central and eastern New Mexico. In Figure 15, the position of each magnetostratigraphic column along the horizontal was determined by (1) the age range indicated in the original reference, (2) the location within the section of a particular stage boundary (e.g., Carnian-Norian), (3) previously published magnetostratigraphic correlations, and/or (4) lithostratigraphic correlations of the Moenkopi and Chinle Formations in the southwestern United States (such as those of Figure 3). The main elements of correlation for the construction of the magnetic polarity sequence are (1) correlation of the polarity sequence of the Chugwater [*Shive et al.*, 1984] and lower Moenkopi [*Helsley and Steiner*, 1974] formations with Early Triassic results from southern China [*Steiner et al.*, 1989; *Heller et al.*, 1988]; (2) correlation of the Middle Triassic polarity sequence of the upper-Moenkopi Formation [*Elston and

TABLE 4. (continued).

Craton (other)	Lat.	Long.	k	α_{95}	Reference
Piedmont dikes, NC	62	55	14	8	19 PD
Chinle, Redonda, NM	58	79	62	4	20 CHr
Manicouagan, Queb.	60	89	58	5	21 MS
Chinle, up. shale, NM	57	88	60	5	22 CHus
Popo Agle, WY	56	96	14	14	23 PA
Ankareh, WY	51	105	143	4	24 A
	49	105	751	5	23 UC
Up. Chugwater, WY	46	121	170	7	23 LC
Lo. Chugwater, WY	47	114	999	2	25 C1
Chugwater, WY	45	115	47	4	26 C2
Chugwater, WY					

Purucker, 1979; this study] with results from eastern Spain [*Turner et al.*, 1989]; (3) correlation of the magnetic polarity sequence within the Chinle Formation in central and eastern New Mexico with the Newark Supergroup in Carnian-Norian times [*Witte and Kent*, 1989; *Olsen and Kent*, 1990]; (4) correlation of the Shinarump/Bluewater Creek (unnamed) member sequence with a preliminary polarity sequence from eastern Greenland [*Reeve et al.*, 1974]. We have also incorporated data from a section we sampled in northeastern New Mexico at Montezuma Gap in the southern Sangre de Cristo Mountains [*Molina-Garza*, 1991]. A brief discussion of the geologic setting of the data used to construct Figure 15 is presented in the appendix.

A well-defined magnetic polarity sequence derived from stable magnetizations in Lower Triassic carbonates and clastics from Sichuan Province (southern China) has been recently reported by *Steiner et al.* [1989]. The section studied by these authors is about 1000 m thick, and contains abundant Early Triassic conodont fauna indicative of an Early Triassic age. The Griesbachian portion of the section is predominantly of normal polarity, as suggested also by *Heller et al.* [1988]. The upper half of the section (Nammalian and Spathian stages), was sampled with lesser detail, yet it is predominantly reversely magnetized with three relatively short lived normal events.

Magnetostratigraphic sequences in Triassic rocks in North America have been obtained only from continental detrital rocks, which generally lack sufficient biostratigraphic control. *Helsley* [1969], *Shive et al.* [1984], and *Steiner et al.* [1989] have suggested a general correlation between the Early Triassic Moenkopi and Chugwater formations based on their magnetostratigraphy. The Red Peak Member of the Chugwater Formation was studied by *Shive et al.* [1984] in central and western Wyoming. Those rocks are characterized by a predominantly reverse polarity state interrupted by relatively short lived normal intervals, a pattern remarkably similar to the one observed in the upper half of the Sichuan section. If the Chugwater and Sichuan sections are correlative it implies that the top of the Red Peak Member of the Chugwater (the Alcova Limestone) is located at about the Nammalian-Spathian stage boundary.

Studies in the Moenkopi Formation are handicapped by problems of correlation between the predominantly reverse section in Utah and Colorado [*Helsley and Steiner*, 1974] with the predominantly normal section in Arizona [*Purucker et al.*, 1980], plus the apparent obliteration of the record by unstable magnetizations in the Ali Baba Member of the formation in Colorado [*Helsley and Steiner*, 1974]. In their 1984 paper, Shive et al. hinted that the overall resemblance of the Moenkopi and Chugwater magnetic polarity sequences is not compelling. Nonetheless, they have supported the tentative correlation proposed by *Helsley* [1969] and *Steiner* [1988]. The correlation preferred by *Steiner* [1988] makes the Chugwater's Red Peak Member equivalent to the entire Moenkopi Formation, whereas the Sewemup member of the Moenkopi in Colorado would be equivalent to the Wupatki Member of the Moenkopi in Arizona. The latest Early Triassic record from Sichuan does not contain sufficient detail either to support or reject the validity of such correlation. However, a magnetic polarity sequence from Spain [*Turner et al.*, 1989] indicates periods of predominantly normal polarity in the Nammalian and in the Spathian-early Anisian, which we think correlate with normal polarity periods in the Moenkopi (the Moqui and Wupatki members in Arizona, and the lower portion of the Moenkopi section in central New Mexico and the Anton Chico Formation in eastern New Mexico). This is supported by the biostratigraphic correlation of the Parriot Member of the Moenkopi Formation (in Colorado) with the lower portion of the Moenkopi in Arizona (Wupatki and Moqui members) and the correlation of the Holbrook Member in Arizona with the Moenkopi strata in central New Mexico.

The Carnian portion of the Late Triassic sequence is mostly constrained by our results from New Mexico. They provide the link between the relatively well-established Early Triassic magnetic polarity sequence, and the recently published Norian sequence in the Passaic Formation of the Newark Supergroup [*Olsen and Kent*, 1990]. The Passaic polarity sequence is predominantly reversely magnetized and shows some similarity with the Redonda Formation results of *Reeve and Helsley* [1972], although the reliability of some of the short normal intervals in the Redonda section is questionable.

Certainly our proposed magnetic polarity time scale needs further refinement but it provides a basic framework which can be tested with future data from Triassic sections where additional biostratigraphic control exists.

CONCLUSIONS

Thermal and chemical demagnetization techniques reveal four components of magnetization in Triassic strata of central New Mexico. The oldest component is interpreted as an early-acquired ("primary") chemical remanent magnetization (CRM) based on a positive micro-conglomerate test and bedding-parallel magnetic polarity zonation. A Late Mesozoic (Cretaceous?) remagnetization is pervasive throughout some stratigraphic intervals. The age of this component of magnetization is constrained by a positive fold test. The mechanism of remagnetization is not fully understood but it may well be related to the migration of fluids during Laramide orogenic activity. A third component of magnetization in the direction of the present dipole field partially overprints the

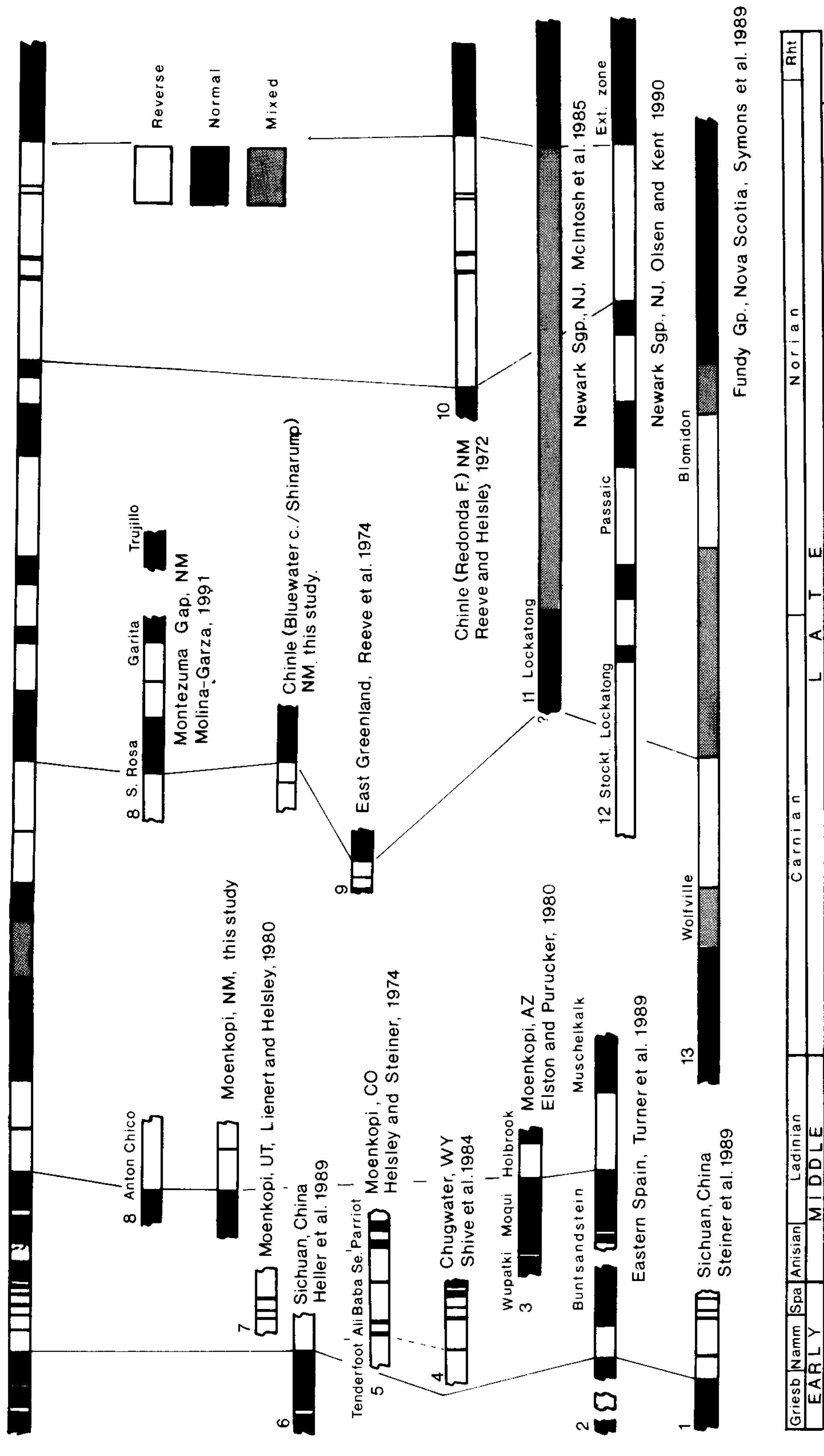

Fig. 15. Preliminary Triassic magnetic polarity time scale. Period boundaries as in *Harland et al.* [1989] time scale.

ancient components. Lastly, we have interpreted a generally lower stability component, characterized by an aberrant easterly direction, as a complex composite magnetization which resulted from mixing of both ancient and late diagenetic magnetizations carried by a magnetic fraction with coercivity, laboratory unblocking temperature, and solubility spectra which may or may not overlap with the spectra of "primary" or other "secondary" carriers.

Based on the characteristic direction of magnetization, we have determined short magnetic polarity sequences which we correlate throughout this area. We also compare these sequences with other Triassic data in order to construct a magnetic polarity time scale for the entire Triassic. Our paleomagnetic pole determination for the Moenkopi Formation is statistically indistinguishable from previous results obtained for the Moenkopi in both Arizona and Colorado. Thus it confirms the general reliability of paleolatitude determinations in previous studies. The paleomagnetic data suggest that portions of central New Mexico have experienced a small clockwise rotation with respect to cratonic North America, similar to that of the Colorado Plateau. Taking such rotations into account, the paleopole for the Chinle Formation Shinarump Member is in excellent agreement with other North American Carnian age poles. Paleopoles for stratigraphic units assigned to the Chinle Formation document a period of about 12° (great circle) of apparent polar wander along a uniform westerly trending path which includes other cratonic poles of similar age.

APPENDIX

1. This entry corresponds to section HPT of *Steiner et al.* [1989]. These authors sampled a 900 m sequence of carbonates of the Feixianguan and Jialingjiang Formations in the Sichuan province of southern China. The Feixianguan Formation contains diagnostic conodont fauna of Griesbachian age. The overlying Jialingjiang Formation contains conodonts which are known from the Nammalian and Spathian stages and is disconformably overlain by Middle Triassic units.

2. *Turner et al.* [1989] reported a magnetic polarity sequence for a stratigraphic section of red beds and conglomerates comprising the Autunian, Saxonian, Buntsandstein, and Muschelkalk, from the Iberian Cordillera in eastern Spain. The Buntsandstein facies is about 550 m in thickness. The base of the Buntsandstein contains Thuringian microflora. The Buntsandstein has been subdivided into six stratigraphic units ranging in age from Thuringian to Ladinian on the basis of palynological assemblages. The Muschelkalk facies have been assigned a Late Ladinian-Early Carnian age.

3. This entry was taken from *Purucker et al.* [1980], who reported paleomagnetic results for the Wupatki, Moqui, and Holbrook members (in ascending stratigraphic order) of the Moenkopi Formation in Arizona. The Holbrook and Moqui members contain Middle Triassic vertebrate fauna [*Morales*, 1987]. The total thickness of the section is 120 m.

4. *Shive et al.* [1984] reported the magnetostratigraphy of a about 200 meters of the Red Peak Member of the Chugwater Formation in Wyoming, in the western United States. The Chugwater disconformably overlies the Late Permian Dinwoody Formation. It consists of red beds and lacks diagnostic fossils, yet, it has been assigned an Early Triassic age based on litho-stratigraphic correlations.

5. *Helsley and Steiner* [1974] and *Helsley* [1969] studied the magnetostratigraphy of an approximately 250 m thick sequence of red beds of the Early-Middle Triassic Moenkopi Formation in western Colorado. The formation has been subdivided in four members (from bottom to top): the Tenderfoot, the Ali Baba, the Sewemup, and the Parriot Member. The Parriot Member has been tentatively correlated with the exposures of the Moenkopi in Arizona and has been assigned to the Middle Triassic (Anisian?).

6. *Heller et al.* [1988] reported the magnetostratigraphy of the Permo-Triassic boundary section in the Sichuan province of southern China. The Triassic portion of the section sampled (the Feixianguan Formation) is about 80 meters in thickness, and it is mostly composed of limestone. The Feixianguan Formation has a well established Griesbachian age, as discussed above. The Permo-Triassic boundary is recognized by a clay horizon rich in iridium, and the extinction of all non-fusulinid foraminifera and radiolaria.

7. This entry was reported by *Lienert and Helsley* [1980]. A magnetic polarity sequence was obtained by these authors for a 80 m thick sequence of red beds of the Moenkopi Formation sampled at Bears Ears in southeastern Utah.

8. These entries are based on data which we have obtained from a Triassic section exposed north of Las Vegas in northeastern New Mexico, at Montezuma Gap [*Molina-Garza*, 1991]. The Anton Chico Formation has been correlated with the Moenkopi Formation in central New Mexico and is of Middle Triassic age. The rest of the section corresponds to the Late Triassic Santa Rosa, Garita Creek, and Trujillo Formations described in the text. Using fossil vertebrates and palynologic data, *Lucas and Hunt* [1989b] have suggested that the Carnian-Norian boundary lies between the upper layers of the Garita Creek Formation (lower Petrified Forest) and the Bull Canyon Formation (upper Petrified Forest) of the Tucumcari basin. We have thermally demagnetized 4 to 6 samples from 28 sites; the majority of the samples yield shallow magnetizations (northerly and southerly) carried by hematite. The section sampled is about 100 m in thickness.

9. Entry number 9 was reported by *Reeve et al.* [1974]. These authors studied the Malmros klint member of the Fleming Fjord Formation of East Greenland. The age of the Malmros klint member is bracketed in the Carnian-Norian age range. The section is approximately 200 m thick, but results were only obtained for a 12 m long core in the lower middle portion of the Malmros klint member. Fossil phyllopods from the base of the Malmros klint are of lowermost Late Triassic age.

10. This entry was reported by *Reeve and Helsley* [1972]. These authors reported a magnetic polarity sequence for a 133 m thick section of the uppermost portion of the Chinle Formation, formerly the Redonda Member but now Redonda Formation, from eastern New Mexico. The age of this unit has been previously discussed in the text.

11. *McIntosh et al.* [1985] published a summary of the magnetostratigraphy of the Newark Supergroup of the northeastern United States. Ages assigned were based on biostratigraphic data. The total thickness of the composite section reported by these authors is 5 km.

12. This entry supersedes in part entry 11. It is based on data for the Newark Supergroup presented by *Olsen and Kent* [1990], which includes data obtained by *Witte and Kent* [1989, 1990]. The section reported by *Olsen and Kent* [1990] is more than 6 km in thickness. The Carnian-Norian boundary has been placed within the lower part of the Passaic Formation. The extrusive interval of the Newark Supergroup has been assigned to the

Lower Jurassic (Hettangian) based on radiometric dating and paleontological data [*Olsen et al.*, 1987].

13. *Symons et al.* [1989] reported paleomagnetic and magnetostratigraphic data for the rift-basin deposits of the Fundy Group in Nova Scotia and New Brunswick. The Fundy Group in Nova Scotia comprises the Wolfville and Blomidon formations. Their combined thickness exceeds 3 km. The age of the Fundy Group is not well established, however, the Wolfville Formation contains reptilian remains that indicate a Middle Triassic (Ladinian) to lower Late Triassic (Carnian) age. The minimum age for the Blomidon formation is set by a 191 +/- 2 Ma K-Ar age obtained for the overlying North Mountain basalts.

Acknowledgments. Financial assistance for the present study was provided by Sigma Xi, the Scott Turner Fund of the University of Michigan, and the New Mexico Bureau of Mines and Mineral Resources. We appreciate permission to conduct field sampling on the Sevilleta Wildlife Refuge. We wish to thank Yianping Li for assistance in the field, Dongowoo Suk and Antonio Arribas for their collaboration on the SEM observations, and Rex Johnson for helpful discussion and comments. The manuscript was greatly improved by comments of the JGR's reviewers. Part of the laboratory expenses were underwritten by a grant from the Division of Earth Sciences, the National Science Foundation, grant EAR 89-05811.

REFERENCES

Ash, S.R., Upper Triassic floral zones of North America, in *Biostratigraphy of Fossil Plants: Successional and Paleoecological Analysis*, edited by D.L. Dilcher and T.N. Taylor, 259 pp., chap. 5, Dowden, Hutchinson, and Ross, Stroudsburg, Pa, 1980.

Baag, C.G., and C.E. Helsley, Evidence for penecontemporaneous magnetization of the Moenkopi Formation, *J. Geophys. Res., 79*, 3308-3320, 1974.

Bailey, R.C., and H.C. Halls, Estimate of confidence in paleomagnetic directions derived from mixed remagnetized circle and direct observational data, *J. Geophys., 54*, 174-182, 1984.

Bazard, D.R., and R.F. Butler, Paleomagnetism of the Chinle Formation, Arizona and New Mexico: Implications for Late Triassic-Early Jurassic apparent polar wander (abstract), *Eos, Trans. AGU*, 70, 1068, 1989.

Bazard, D.R., and R.F. Butler, Late Triassic-Early Jurassic APW: A view from the southwestern United States (abstract), *Eos Trans. AGU, 71*, 489, 1990.

Beck, M.E., Paleomagnetism of Upper Triassic diabase from southeastern Pennsylvania: Further results, *J. Geophys. Res., 77*, 5673, 1972.

Brown, L.L., and M.P. Golombek, Tectonic rotations within the Rio Grande rift, New Mexico: Evidence from paleomagnetic studies, *J. Geophys. Res., 90*, 790-802, 1985.

Bryan, P., and R.G. Gordon, Rotation of the Colorado Plateau: analysis of paleomagnetic data, *Tectonics, 5*, 661-667, 1986.

Bryan, P., and R.G. Gordon, Rotation of the Colorado Plateau: an updated analysis of paleomagnetic data (abstract), *Geol. Soc. Am. Abstr. Programs, 20*, A63, 1988.

Clark, J.M., and D.E. Fastovsky, Vertebrate biostratigraphy of the Glen Canyon Group in Arizona, in *The Age of the Dinosaurs*, edited by K. Padian, pp. 285-301, Cambridge University Press, New York, 1986.

Collinson, D.W., The role of pigment and specularite in the remanent magnetization of red sandstones, *Geophys. J. R. Astron. Soc., 62*, 393-402, 1974.

Demarest, H.H., Error analysis for the determination of tectonic rotation from paleomagnetic data, *J. Geophys. Res., 88*, 4321-4328, 1983.

Diehl, J.F., and P.N. Shive, Paleomagnetic results from the Late Carboniferous/Early Permian Casper Formation: Implications for Northern Appalachian tectonics, *Earth Planet. Sci. Lett., 54*, 281-292, 1981.

Dooley, R.E., and W.A. Smith, Paleomagnetism of Early Mesozoic dikes in the South Carolina Piedmont, *Tectonophysics, 90*, 283-307, 1982.

Ekstrand, E.J., and R.F. Butler, Paleomagnetism of the Moenave Formation: Implications for the Mesozoic North American apparent polar wander path, *Geology, 17*, 245-248, 1989.

Elston, D.P., and M.E. Purucker, Detrital magnetization in red beds of the Moenkopi Formation (Triassic), Gray Mountain, Arizona, *J. Geophys. Res., 84*, 1653-1665, 1979.

Fang, W., and R. Van der Voo, Paleomagnetism of Middle-Late Triassic plutons in southern Maine, *Tectonophysics*, 156, 51-58, 1988.

Fisher, N.I., T. Lewis, and M.E. Wilcox, Tests of discordancy for samples from Fisher's distribution on the sphere, *Appl. Statist., 30*, 230-237, 1981.

Geissman, J.W., S.S. Harlan, and A.J. Brearley, The physical isolation and identification of carriers of geologically stable remanent magnetization: paleomagnetic and rock magnetic microanalysis and electron microscopy, *Geophys. Res. Lett., 15*, 479-482, 1988.

Gordon, R.G., A. Cox, and S. O'Hare, Paleomagnetic Euler poles and the apparent polar wander and the absolute motion of North America since the Carboniferous, *Tectonics, 3*, 499-537, 1984.

Grubbs, K.L., and R. Van der Voo, Structural deformation of the Idaho-Wyoming Overthrust Belt (U.S.A.), as determined by Triassic paleomagnetism, *Tectonophysics, 33*, 321-336, 1976.

Harland, W.B., R.L. Armstrong, A.V. Cox, L.E. Craig, A.G. Smith, and D.G. Smith, *A Geologic Time Scale 1989*, Cambridge University Press, New York, 1989.

Hayden, S.N., and C.K. Mawer, Dextral transtensional deformation along the western margin of the Rio Grande rift, central New Mexico, (abstract), *Geol. Soc. Am. Abstr. Programs, 23*, A31, 1991.

Heller, F., W. Lowrie, L. Huamei, and W. Junda, Magnetostratigraphy of the Permo-Triassic boundary section at Shangsi (Guangyuan), Sichuan Province, China, *Earth Planet. Sci. Lett., 88*, 348-356, 1988.

Helsley, C.E., Magnetic reversal stratigraphy of the Lower Triassic Moenkopi Formation of Western Colorado, *Geol. Soc. Am. Bull., 80*, 2431-2450, 1969.

Helsley, C.E., and M.B. Steiner, Paleomagneti of the Lower Triassic Moenkopi Formation, *Geol. Soc. Am. Bull., 85*, 457-464, 1974.

Herrero-Bervera, E., and C.E. Helsley, Paleomagnetism of a polarity transition in the Lower (?) Triassic Chugwater Formation, Wyoming, *J. Geophys. Res., 88*, 3506-3522, 1983.

Hunt, A.P., and S.G. Lucas, Late Triassic vertebrates from the Los Esteros Member, Santa Rosa Formation, east-central New Mexico, *J. Vertebrate Paleont., 8*, 18, 1988a.

Hunt, A.P., and S.G. Lucas, Triassic stratigraphy, Carthage area, Socorro County, New Mexico and the southeasternmost outcrops of the Moenkopi Formation, *N. M. Geol., 10*, 45, 1988b.

Hunt, A.P., S.G. Lucas, and P.L. Sealy, Paleontology and vertebrate biochronology of the Upper Triassic Garita Creek Formation, east-central New Mexico, *N. M. J. Sci., 29*, 61-68, 1989.

Irving, E., and M.R. Banks, Paleomagnetic results from the Upper Triassic lavas of Massachusetts, *J. Geophys. Res., 66*, 1935-1939, 1961.

Irving, E., E. Tanczyk, and J. Hastie, *Catalogue of Paleomagnetic Directions and Poles, Geomagn. Ser., 6*, Energy, Mines, and Resources, Canada, Ottawa, Canada, 1976.

Jackson, M., and R. Van der Voo, Thermally activated viscous remanence in some magnetite- and hematite-bearing dolomites, *Geophys. Res. Lett., 13*, 1434-1437, 1986.

Johnson, A.H., and A.E.M. Nairn, Jurassic paleomagnetism, *Nature, 240*, 551-552, 1972.

Kelley, V.G., Tectonics, middle Rio Grande rift, New Mexico, in *Rio Grande Rift Tectonics and Magmatism*, edited by R. E. Riecker, pp. 57-70, AGU, Washington, D.C., 1979.

Kietzke, K.K., Calcareous microfossils from the Moenkopi Formation (Triassic, Scythian or Anisian) of central New Mexico, *Field Conference Guidebook N.M. Geol. Soc. 40*, 181-190, 1989.

Kirschvink, J.L., The least squares line and plane and analysis of paleomagnetic data, *Geophys. J. R. Astron. Soc., 45*, 699-718, 1980.

Larson, E.E., and T.R. Walker, A rock magnetic study of the Lower Massive Sandstone, Moenkopi Formation (Triassic), Gray Mountain area, Arizona, *J. Geophys. Res., 87*, 4819-4836, 1982.

Larson, E.E., T.R. Walker, P.E. Patterson, R. P. Hoblitt, and J. Rosenbaum, Paleomagnetism of the Moenkopi Formation, Colorado Plateau: Basis for long-term model of acquisition of CRM, *J. Geophys. Res., 87*, 4819-4836, 1982.

Lienert, B.R., and C.E. Helsley, Magnetostratigraphy of the Moenkopi Formation at Bears Ears, Utah, *J. Geophys. Res., 85*, 1475-1480, 1980.

Lucas, S.G., and S.N. Hayden, Late Triassic lake in central New Mexico, in *Abstracts of the Symposium on Southwestern Geology and Paleontology*, p. 12, Museum of Northern Arizona, Flagstaff, 1988.

Lucas, S.G., and S.N. Hayden, Triassic stratigraphy of west-central New Mexico, in *Field Conf. Guideb. N.M. Geol. Soc., 40*, Southeastern Colorado Plateau, 191-212, 1989.

Lucas, S.G., and A.P. Hunt, Stratigraphy of the Anton Chico and Santa Rosa Formations, Triassic of east-central New Mexico, *J. Ariz.-Nev. Acad. Sci., 22*, 21-33, 1987.

Lucas, S.G., and A.P. Hunt, Vertebrate Bichronology of Late Triassic, *28th International Geological Congress (Washington, D.C.) Abstracts*, vol. 2, pp. 335-336, International Union Geological Scientists, Washington, D.C., 1989a.

Lucas, S.G., and A.P. Hunt, Revised Triassic stratigraphy in the Tucumcaribasin, east-central New Mexico, in *Dawn of the age of the Dinosaurs in the American Southwest*, edited by S.G. Lucas and A.P. Hunt, pp. 150-170, New Mexico Museum of Natural History, Albuquerque, 1989b.

Lucas, S.G., A.P. Hunt, and M. Morales, Stratigraphic nomenclature and correlation of Triassic rocks of east-central New Mexico: a preliminary report, *Field Conf. Guideb. N.M. Geol. Soc., 36*, 199-203, 1985.

Lucas, S.G., K.K. Kietzke, S.N. Hayden, and B. Allen, Triassic strata in the Hubbel Springs fault zone, Valencia County, New Mexico, *N. M. Geol., 10*, 65, 1988.

Lupe, R., and N.J. Silberling, Genetic relationship between Lower Mesozoic continental strata of the Colorado Plateau and marine strata of the western Great Basin: significance for accretionary history of Cordilleran lithotectonic terranes, in *Tectonostratigraphic Terranes of the Circum-Pacific Region*, edited by D.G. Howell, pp. 263-270, Circum-Pacific Council for Energy and Mineral Resources, Houston, Texas, 1985.

Manning, A.H., and J.Z. de Boer, Deformation of Mesozoic dikes in New England, *Geology, 17*, 1016-1019, 1989.

May, S.R., and R.F. Bulter, North American Jurassic Apparent Polar Wander: Implications for plate motion, paleogeography, and Cordilleran tectonics, *J. Geophys. Res*, 91, 11,519 - 11,544, 1986.

McFadden, P.L., and M.W. McElhinny, Classification of the reversal test in paleomagnetism, *Geophys. J. Int*, in press, 1990.

McIntosh, W.C., R.B. Hargraves, and C.L. West, Paleomagnetism and oxide mineralogy of Upper Triassic to Lower Jurassic red beds and basalts in the Newark Basin, *Geol. Soc. Am. Bull., 96*, 463-480, 1985.

McMahon, B.E., and D.W. Strangway, Stratigraphic implications of paleomagnetic data from Upper Paleozoic-Lower Triassic red beds of Colorado, *Geol. Soc. Am. Bull., 79*, 417-428, 1969.

Molina-Garza, R.S., Permian and Triassic paleomagnetism from Mexico and the southwestern United States: Implications for the evolution of the Gulf of Mexico and the Magnetic Polarity Time Scale, Ph.D. Thesis, University of Michigan, Ann Arbor, 1991.

Molina-Garza, R.S., J.W. Geissman, and R. Van der Voo, Paleomagnetism of the Dewey Lake Formation, northwest Texas: End of the Kiaman Superchron in North America, *J. Geophys. Res., 94*, 17,881-17,888, 1989.

Morales, M., Terrestrial fauna and flora from the Triassic Moenkopi Formation of the southwest United States, *J. Ariz.-Nev. Acad. Sci., 22*, 1-19, 1987.

Olsen, P.E., and D.V. Kent, Continental coring of the Newark Rift, *Eos, Trans. AGU, 71*, 385, 394, 1990.

Olsen, P.E., and R.W. Schlische, Transtensional arm of the Mesozoic Fundy rift basin: Penecontemporaneous faulting and sedimentation, *Geology, 18*, 695-698, 1990.

Olsen, P.E., N.H. Shubin, and M.H. Anders, New Early Jurassic Tetrapod assemblages constrain Triassic-Jurassic Tetrapod extinction event, *Science, 237*, 1025-1029, 1987.

Peterson, D.N., and A.E.M. Nairn, Paleomagnetism of Permian red beds from the southwest United States, *Geophys. J. R. Astron. Soc., 23*, 191-206, 1971.

Purucker, M.E., D.P. Elston, and E.M. Shoemaker, Early acquisition of characteristic magnetization in red beds of the Moenkopi Formation (Triassic), Gray Mountain, Arizona, *J. Geophys. Res., 85*, 997-1012, 1980.

Reeve, S.C., Paleomagnetic studies of sedimentary rocks of Cambrian and Triassic age, Ph.D. Dissertation, Univ. of Texas at Dallas, 1975.

Reeve, S.C., and C.E. Helsley, Magnetic reversal sequence in the upper portion of the Chinle Formation, Montoya, New Mexico, *Geol. Soc. Am. Bull., 83*, 3795-3812, 1972.

Reeve, S.C., D. Leythaeuser, Helsley, C.E., and K.W. Bay, Paleomagnetic results from the Upper Triassic of East Greenland, *J. Geophys. Res., 79*, 3302-3307, 1974.

Runcorn, S.K., Paleomagnetic surveyin Utah and Arizona: Preliminary results, *Geol. Soc. Am. Bull., 67*, 301-316, 1956.

Seguin, M. K., K.V. Rao, and D.V. Venugopal, Paleomagnetism of parts of the Late Triassic diabase dike system associated with the trans-New Brunswick aeromagnetic lineament, *Can. J. Earth Sci., 18*, 1776-1787, 1981.

Shive, P.N., M.B. Steiner, and D.T. Huycke, Magnetostratigraphy, paleomagnetism, and remanence acquisition in the Triassic Chugwater Formation of Wyoming, *J. Geophys. Res., 89*, 1801-1815, 1984.

Smith, T.E., and H.C. Noltimier, Paleomagnetism of the Newark trend igneous rocks of the north central Appalachians and the opening of the Central Atlantic Ocean, *Am. J. Sci., 279*, 778-807, 1979.

Steiner, M.B., Rotation of the Colorado Plateau, *Tectonics, 5*, 649-660, 1986.

Steiner, M.B., Paleomagnetism of the Late Pennsylvanian and Permian: A test for the rotation of the Colorado Plateau, *J. Geophys. Res., 93*, 2201-2215, 1988.

Steiner, M.B., and C.E. Helsley, Magnetic polarity sequence of the Upper Triassic Kayenta Formation, *Geology, 2*, 191-194, 1974.

Steiner, M.B., J.G. Ogg, Z. Zhang, and S. Sun, The Late Permian-Early Triassic magnetic polarity time scale and plate motions of south China, *J. Geophys. Res., 94*, 7343-7363, 1989.

Stewart, J.H., F.G. Poole, and R.F. Wilson, Stratigraphy and origin of the Chinle Formation and related Upper Triassic strata in the Colorado Plateau region, *U.S. Geol. Surv. Prof. Pap., 690*, 336 pp., 1972*a*.

Stewart, J.H., F.G. Poole, and R.F. Wilson, Stratigraphy and origin of the Triassic Moenkopi Formation and related strata in the Colorado Plateau region, *U.S. Geol. Surv. Prof. Pap., 691*, 195 pp., 1972*b*.

Symons, D.T.A., Early Permian pole evidence from the Pictou red beds, Prince Edward Island, Canada, *Geology, 18*, 234-237, 1990.

Symons, D.T.A., R.E. Bormann, and R.P. Jans, Paleomagnetism of the Triassic red beds of the lower Fundy Group and Mesozoic tectonism of the Nova Scotia platform, Canada, *Tectonophysics, 164*, 13-24, 1989.

Turner, P., Relationship between magnetic components and diagenetic features in reddened Triassic alluvium (St. Bees Sandstone, Cumbria, UK), *Geophys. J. R. Astron. Soc., 67*, 395-413, 1981.

Turner, P., A. Turner, A. Ramos, and A. Sopena, Paleomagnetism of Permo-Triassic rocks in the Iberian Cordillera, Spain: acquisition of secondary and characteristic remanence, *J. Geol. Soc. London, 146*, 61-76, 1989.

Van der Voo, R., Phanerozoic paleomagnetic poles from Europe and North America and comparisons with continental reconstructions, *Rev. Geophys., 28*, 167-206, 1990.

Van der Voo, R., and K.L. Grubbs, Paleomagnetism of the Chugwater red beds revisited (Wyoming, U.S.A.), *Tectonophysics, 44*, T27-T33, 1977.

Van Fossen, M.C., J.J. Flynn, and R.D. Forythe, Paleomagnetism of Early Jurassic rocks, Watchung Mountains, Newark Basin: Evidence for complex rotations along the border fault, *Geophys. Res. Lett., 13*, 185-188, 1986.

Walker, T.R., E.E. Larson, and R.P. Hoblitt, Nature and origin of hematite in the Moenkopi Formation (Triassic), Colorado Plateau: a contribution to the origin of magnetism in red beds, *J. Geophys. Res.*, *86*, 317-333, 1981.

Witte, W.K., and D.V. Kent, A middle Carnian to early Norian (225 Ma) paleopole from sediments of the Newark Basin, Pennsylvania, *Geol. Soc. Am. Bull.*, *101*, 1118-1126, 1989.

Witte, W.K., and D.V. Kent, The paleomagnetism of red beds and basalts of the Hettangian extrusive zone, Newark Basin, New Jersey, *J. Geophys. Res.*, *95*, 17,533-17,546, 1990.

Zijderveld, J.D.A., A.C. demagnetization of rocks: Analysis of results, in *Methods In Palomagnetism*, edited by D.W. Collinson, K.M. Creer, and S.K. Runcorn, pp. 245-286, Elsevier, New York, 1967.

J.W. Geissman and S.N. Hayden, Department of Geology, University of New Mexico, Albuquerque, N.M 87131-1116.

S.G. Lucas, New Mexico Museum of Natural History, Albuquerque, N M 87104.

R.S. Molina-Garza and R. Van der Voo, Department of Geological Sciences, University of Michigan, Ann Arbor, MI 48109-1063.

(Received July 12, 1990;
revised February 26, 1991;
accepted February 26, 1991.)